Opto-Electronic
Advances

CN 51–1781/TN ISSN 2096–4579 (Print) ISSN 2097–3993 (Online)

The possibilities of using a mixture of PDMS and phosphor in a wide range of industry applications

Rodrigo Rendeiro, Jan Jargus, Jan Nedoma, Radek Martinek and Carlos Marques

Citation: Rendeiro R, Jargus J, Nedoma J, et al. The possibilities of using a mixture of PDMS and phosphor in a wide range of industry applications. *Opto-Electron Adv* **7**, 240133(2024).

https://doi.org/10.29026/oea.2024.240133

Received: 2 June 2024; Accepted: 19 August 2024; Published online: 20 September 2024

Opto-Electronic Advances

Review

November 2024, Vol. 7, No. 11

DOI: 10.29026/oea.2024.240133 CSTR: 32247.14.oea.2024.240133

The possibilities of using a mixture of PDMS and phosphor in a wide range of industry applications

Rodrigo Rendeiro[1], Jan Jargus[2], Jan Nedoma[2], Radek Martinek[3] and Carlos Marques[1,4*]

A mixture of polydimethylsiloxane (PDMS) doped with phosphor particles can be found across diverse industries having different applications. This mixture plays a particularly important role in the field of lighting, white light-emitting diodes (LED's), flexible display devices, anti-counterfeiting (AC) solutions, luminescence thermometers and many types of sensors. The field of mechanoluminescence and biomedical are booming and there is also potential for visible light communication (VLC). In this comprehensive review, the basic characteristics of PDMS and a list of selected phosphors suitable for creating a mixture of PDMS and phosphor are presented. The summary and a detailed overview of the implemented applications of this perspective mixture over the last decade is presented as well.

Keywords: PDMS; phosphor; white LED's; display; flexible light devices; anti-counterfeiting; luminescence thermometry; visible light communication; mechanoluminescence

Rendeiro R, Jargus J, Nedoma J et al. The possibilities of using a mixture of PDMS and phosphor in a wide range of industry applications. *Opto-Electron Adv* **7**, 240133 (2024).

Introduction

The combination of phosphor and polydimethylsiloxane (PDMS) is constantly finding new possibilities for its application in many areas of human activity and industrial production. This is due to the fact that the mixture of phosphorus and PDMS has many advantageous properties. PDMS is an elastomeric polymer first synthesised in the 1950s by Wacker Chemies and the first main use was the encapsulation of electronic components, acting as a dielectric insulator, protecting the components from mechanical shocks and other environmental factors within a large temperature range. Due to its high elasticity and stability of its properties, PDMS is widelly used as mechanical sensor[1,2].

In 1998, a patent describing the use of PDMS mixed with phosphorus materials for the optical encapsulation of LED's was filled. In this patent, PDMS is referred as the best alternative to the conventional alternative at the time, polymethylmethacrylate (PMMA), polycarbonate, optical nylon, transfer molded and/or cast epoxy have been used for encapsulation. However, these materials suffered degradation of the optical characteristics over

[1]CICECO – Aveiro Institute of Materials, Physics Department, University of Aveiro, Aveiro 3810-193, Portugal; [2]Department of Telecommunications, VSB – Technical University of Ostrava, Ostrava 70800, Czech Republic; [3]Department of Cybernetics and Biomedical Engineering, VSB – Technical University of Ostrava, Ostrava 70800, Czech Republic; [4]Department of Physics, VSB – Technical University of Ostrava, Ostrava 70800, Czech Republic.

*Correspondence: C Marques, E-mail: carlos.marques@ua.pt

Received: 2 June 2024; Accepted: 19 August 2024; Published online: 20 September 2024

time, contrary to PDMS[3]. Epoxy-based resins tend to yellow over time due to high temperature exposure and absorption of ultraviolet (UV)/blue light[4]. Depending on the choice of phosphor, it is possible to obtain the desired range of excitation and converted wavelengths. A downconversion or upconversion phosphor can be more suitable for a particular application. In the case of upconversion, the excitation wavelength is longer than the converted one, and the opposite is true for downconversion. For combination with phosphor, it is preferable to use clear polydimethylsiloxane, e.g. Sylgard 184 type. Thanks to the clear color, light losses of both excitation and converted light are minimized. PDMS is a chemically stable substance with remarkable resistance to thermal and oxidative degradation and is also resistant to UV and radiation. PDMS has the ability to withstand long-term temperatures in the range of approximately −50 °C to 200 °C and can withstand even higher temperatures for a short time. Due to its bonds, it has high adhesion and is strongly hydrophobic. PDMS elastic modulus can be between 1.32 and 2.97 MPa and tensile strength from 3.51 to 5.13 MPa, depending on the manufacturing method. It also has excellent electrical insulation properties, is resistant to various chemicals, does not cause corrosion of other materials and has gas permeability. PDMS devices usually have repeatability while being easy to manufacture and cost-effective, as with replica moulding. PDMS is biocompatible, with reported uses in microfluids, biomodels, organ-on-a-chip platforms, blood analogues and membranes for filtering[2,5,6]. The connection of phosphor and PDMS therefore leads to considerable resistance of this mixture to the chemical and physical effects of the external environment. At the same time, it maintains flexibility in setting the wavelength ranges of excitation and converted light. In addition, it is a flexible and self-supporting mixture that exhibits sufficient mechanical resistance in many areas of use[7–14]. Among the most important are the area of white-LED's and solid-state lighting, for instance[15–18]. Other important areas include anti-counterfeiting (AC) solutions[19–22], temperature sensors or thermoluminescence[23–26] and mechanoluminescence including also biomedical applications[27–30]. In particular, mechanoluminescence has recently experienced a great boom. The mixture of PDMS and phosphor finds application in many sensor and detection applications[31–34], Fig. 1 summarizes some of the different applications, discussed in more detail in the next sections, where the mixture of PDMS and phosphor materials can be found.

The areas where the blend is most matured are solid-state lighting, specially white-LED's and AC solutions. In contrast, the application in sensing, where the use of the blend has a strong perspective in different areas, has yet to be totally explored. Some of the explored areas in sensing include: pH sensor, bio-sensor (mechanical, using the mechanoluminescence capabilities and thermal, using the thermoluminescence capabilities), metal and/or gaseous particles detector, X-ray and UV detection, etc. And there are certainly opportunities and challenges in the field of visible light communications (VLC)[35–37]. However, many phosphors are used in several areas, and therefore in some cases it is not easy to determine the most important area of application of a given phosphor, for example[38–40], which highlights the versatility of PDMS and phosphor blends.

It is known that a phosphor consists of a host crystal (host lattice) and a luminescence center (activator), so these two components influence the resulting properties of the phosphor. In Table 1 some of the typical host matrix, typical activator ions and respective emissions are showcased.

Different properties of phosphors with Ce^{3+} activator

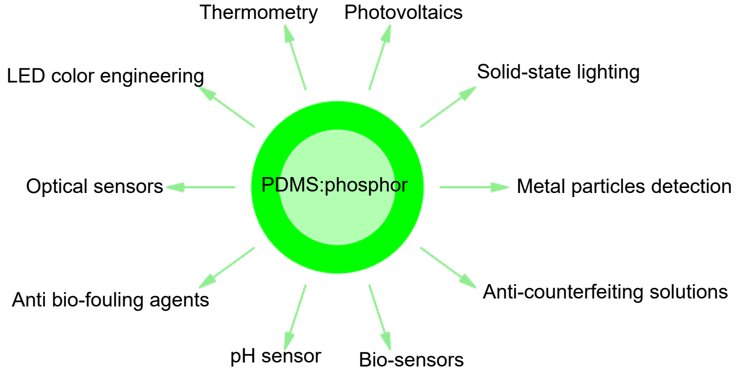

Fig. 1 | Some applications of PDMS:phosphor, highlighting the heterogeneity of applications where the blend has potential uses.

Table 1 | Phosphor Blends of PDMS:host matrix:activator ion and respective wavelengths of emission.

Host matrix	Activator ion	Main emission peak (nm)	Refs.
YAG	Ce	547	ref.[41]
YAG	Eu	480	ref.[42]
YAG	Ce,Gd	571	ref.[43]
ZnS	Cu	516	ref.[44]
ZnS	Mn	585	ref.[45]
ZnS	Ag	450	ref.[46]
$BaLa_2ZnO_5$	Tb	545	ref.[47]
$BaLa_2ZnO_5$	Dy	487	ref.[48]
$BaLa_2ZnO_5$	Eu	705	ref.[49]

located in different types of host crystals (Fluorides, Oxyhalides, Aluminates, Silicates and others) are known[50]. Introducing Gd^{3+} ions, which are larger and thus have a increased crystal field than Y^{3+} causes a red shift of the Ce^{3+} emission in YAG : Ce^{3+}. A substitution of Al^{3+} ions for the larger Gd^{3+} shifts the spectrum in the other direction, due to the weaker crystal field of the Ce^{3+}[51,52].

Typical manufacturing process of PDMS and phosphor mixture

The process of preparing the PDMS phosphor mixture has several stages. Due to its suitable physical and chemical properties, PDMS type Sylgard 184 (Dow company) is very often used. There are many types of PDMS, but Sylgard 184 type PDMS is used very often in practice. It will therefore be presented a possible recommended procedure manufacturing process of PDMS and phosphor mixture for Sylgard 184. For other types of PDMS, the procedure can be similar, however, there can be some specific differences. Sylgard 184 is a two-component silicone elastomer that consists of a "base" and a "curing agent" with a recommended mixing ratio of 10∶1 (base∶curing agent) by weight. After mixing these two components, the mixture is usually stirred briefly and intensively.

As a result of mixing, a large number of air bubbles form in the mixture, which must be removed. To remove the bubbles, either a vacuum chamber is used, or they are allowed to leave on their own. To improve and speed up the process of spontaneous bubble removal, this mixture can be temporarily placed in a refrigerator (e.g. at a temperature of around 5 degrees Celsius). Then comes the phase of mixing PDMS and phosphor in a precisely selected mass ratio, when the required amount of PDMS and powdered phosphor is weighed on precise scales and mixed together, while this mixture is placed in a suitable container, e.g. into a test tube.

Next, the process of homogenization of the PDMS phosphor mixture occurs. This process can be implemented with the help of an ultrasonic bath, or a mechanical shaker, or a combination of both of these options. However, longer-term use of the ultrasonic bath can lead to more intense heating of the PDMS phosphor mixture, which then leads to faster unwanted thermal curing of the mixture. To delay this thermal curing, it is advisable to place the test tube with the PDMS phosphor mixture and the shaker in a cooling box (e.g. with a temperature of around 5 degrees Celsius).

It is advisable that this process of mechanical shaking of the PDMS phosphor mixture takes place for at least 2–3 hours. However, with the use of a cooling box, it is then possible to extend the shaking time of the PDMS phosphor mixture to 10 hours. It seems appropriate to place the test tube with the weighed PDMS phosphor mixture in a shaker that combines the possibility of rotational and vibrational movement, which can be, for example, a rotary shaker of the Multi Bio RS-24 type (Biosan company).

After the end of the phase of homogenization of the PDMS phosphor mixture, it is necessary to place the PDMS phosphor mixture in the desired place. Thin layers of PDMS phosphor mixtures are often created on suitable surfaces (e.g. microscope slides, wafers, etc.) using spin coating or dip coating techniques. Sometimes the possibility of pouring PDMS phosphor mixtures into a suitably shaped container is also used.

Then comes the final phase, which is the thermal curing of the PDMS phosphor mixture. Surfaces with an applied layer of PDMS phosphor or containers into which this mixture was poured are placed in an oven, where they are thermally cured. The specified thermal curing time is dependent on temperature and may also depend on the volume of the PDMS phosphor mixture, on the mass ratio of PDMS : phosphor, on the type of phosphor used, etc. The following values are given in Table 2 for pure PDMS type Sylgard 184 (without phosphor). In addition to the above, each researcher working with a mixture of PDMS phosphors can have their own specific production processes of combining PDMS with phosphors, as well as customized equipment such as their own home-made shaker etc.

Table 2 | Cure time and temperature for PDMS type Sylgard 184[53].

Time (min)	Temperature (°C)
10	150
20	125
35	100

The price of the PDMS phosphor mixture depends on the price of its components and on the weight ratio of PDMS and phosphor. In the case of the most used PDMS type Sylgard 184, the price for 1 kg of Sylgard 184 can be around 160 euros. The price of the frequently used phosphor YAG:Ce^{3+} for white-LED and solid-state lighting can be, for example, around 9 euros per gram of YAG:Ce^{3+}. Using the spin coating technique, it is possible to apply a sufficient layer on the central part of the standard microscope slide with an amount of 0.2 g of the PDMS phosphor mixture. In the case of a considerably large weight ratio of *PDMS* : *phosphor* 2 : 1, the total price for 0.2 g of the *PDMS* : *phosphor* mixture (Sylgard 184: YAG:Ce^{3+}) applied to the central part of the microscope slide can be approx. 0.62 euros (approx. 0.02 euros for PDMS and 0.6 euros for phosphor). Figure 2 displays a photograph from a microscope slide containing the mixture PDMS and YAG:Ce^{3+}.

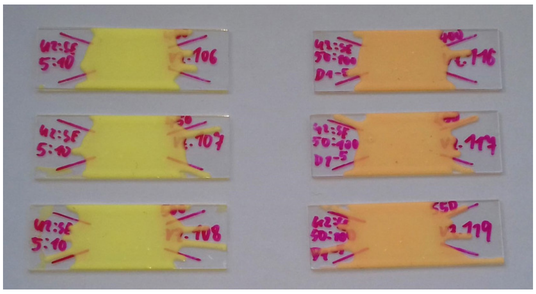

Fig. 2 | Photograph of a microscope slide containing emitting samples with PDMS and YAG:Ce^{3+} (main emission peak at 555 nm) on the left side and the samples on the right side contain PDMS, YAG:Ce^{3+} and CaS:Eu^{2+} (main emission peak at 650 nm), using as excitation source blue light. Figure reproduced from ref.[37], under a Creative Commons Attribution International License.

However, in the case of using another application technique on a microscope slide, e.g. the dip coating technique, the total price of the mixture PDMS phosphor applied to a microscope slide will probably be much higher. This will be caused by the need to mix a large volume of the PDMS phosphor mixture into the container into which the microscope slide will be immersed, and logically most of the PDMS phosphor mixture will remain unused. So the use of the Dip coating technique for applying the PDMS phosphor layer can be quite cost-inefficient.

On the other hand, the application of the PDMS phosphor layers using the spin coating technique also produces waste. This is created by the excess of the PDMS phosphor mixture being transposed onto the inner walls of the spin coater thanks to the forces acting during the rotation of the layer. Even so, the application of layers of the PDMS phosphor mixture using the spin coating technique is much more cost-effective in contrast to the dip coating technique.

Producing very small volumes of PDMS phosphor mixture samples can also be generally cost-inefficient, as it is practically difficult to homogeneously mix a very small volume of PDMS phosphor mixture and at the same time transfer it to the requested location. E.g. larger volumes, on the order of milliliters, are better mixed in the test tube, however, part of this volume will remain inefficiently used due to adhesion to the walls of the test tube.

In section *Applications - PDMS and phosphor* some of the most reported applications such as, white-LED's and solid-state lighting, anti-counterfeiting solutions, temperature sensors, thermoluminescence, mechanoluminiscense and bio-medical are reviewed, with some of its mechanisms and manufacturing methods being explored. In section *Discussion and future perspectives* some of the advantages and disadvantages of using these mixtures are reviewed, as well as future developments.

Applications - PDMS and phosphor

The combination of PDMS and phosphorus creates a mixture that finds application in many industries. The four main areas of application of the *PDMS* : *phosphor* blend were mentioned in the introduction and will be detailed in the following subsections. In addition, there are many other possibilities of using the *PDMS* : *phosphor* mixture, which will be mentioned in a separate subsection.

Individual applications are determined depending on the specific type of phosphorus. When using powdered phosphorus, it is common practice to create a homogeneous mixture of PDMS and phosphorus with an adjustable *PDMS* : *phosphor* weight ratio. PDMS serves as a binder, mechanical protection and is important from the point of view of guiding the excitation radiation to the luminescence centers. For flexible bio-sensors its biocompatibility and hyperelasticity are some highlighted features. In the case of specific applications, such as gas detection, its permeability allows to better sense these environments.

White-LED's and display technology

The most important area for the use of the *PDMS* : *phosphor* mixture is the area of white-LED's and solid-state lighting. These are often phosphors excited by narrowband UV radiation or blue light present in the optical packaging of the chip. In the case of phosphorescent white-LED's, the weight ratio of the mixture is carefully engineered in a way that part of the excitation energy (UV or blue) is converted into a long-wave broadband component and part maintains the short-wave component. The combination of these components causes the emission of white light. Usually, this coating can be either applied mixed in the optical packaging silicone (as in typical commercial white-LED's) (see Fig. 3(a)), on the surface of the LED chip (see Fig. 3(b)) or on the surface of the optical packaging (see Fig. 3(c)). Using the second method reduces backscatering of blue light from the phosphor to the chip, causing reabsorption and reducing the overall luminescence efficiency. However, in commercial applications, the costs due to extra processing make the first a more viable commercial application[54].

The most common phosphor blends for white phosphor LEDs are YAG:Ce^{3+} (yellow emitter activated mainly by 440–480 nm light, with an absorption peak at 460 nm) or a combination of blue/green/red phosphors (activated with 360–410 nm light), such as $BaMgAl_{10}O_{17}:Eu^{2+}/Ba_2SiO_4:Eu^{2+}/CaAlSiN_3:Eu^{2+}$ [56]. YAG:Ce^{3+} is a commercial solution widely used for white-LED's and solid-state lighting. Some authors use different variants of the designation of this phosphor (YAG : Ce; $Y_3Al_5O_{12}:Ce^{3+}$; YAG phosphor). The combination of blue/green/red phosphors can offer superior color quality in exchange for a more complex design of the coating and less efficient power source.

Many issues of phosphors in these applications are temperature quenching and degradation. Several protective measures can be taken to reduce these issues, such as, forming protective surface layers against moisture and high temperature in fluoride and sulphide based phosphors; surface coating in silicate and oxide based phosphors increases its Photoluminescence (PL) efficiencies; surface passivation treatment in nitrite and oxynitride based phosphors, reducing thermal degradation of PL intensity[57].

To note that this technique was already employed in fluorescent lamps, with the latter using as excitement source the UV produced by the eletric discharge in gas enclosed into vacuum tubes. The main criterion to apply a phosphor into an LED for white light is that they must show strong absorption in UV/near-ultraviolet (NUV) while having an efficient emission in the region of visible light. The combination of *PDMS* : *phosphor* allows to easily achieve a white tone using a single LED, contrasting with the red-green-blue (RGB) solution, which

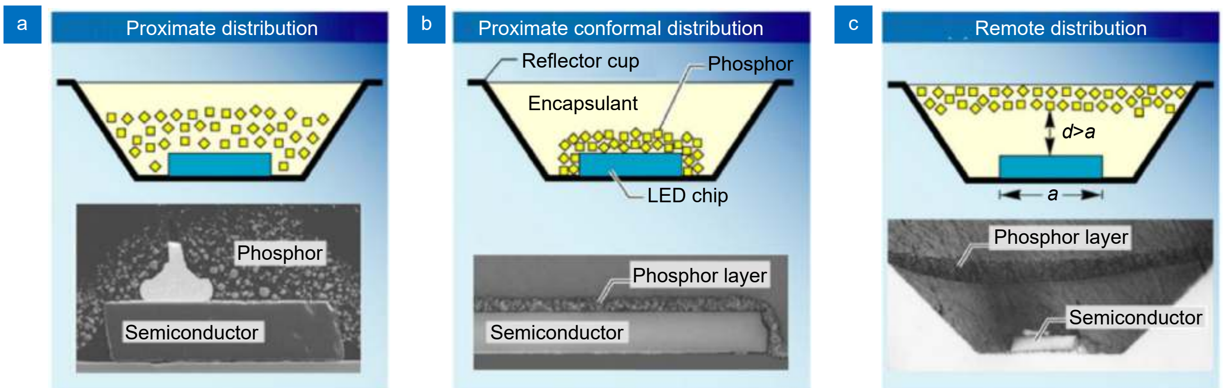

Fig. 3 | Schematic diagram of LED packaging. (**a**) Proximate phosphor configuration, where the phosphor is homogeneously distributed across the optical packaging host. (**b**) Proximate conformal phosphor configuration, with the phosphor deposited on the LED surface. (**c**) Remote phosphor configuration, with the layer of the phosphor on the surface of the host matrix. Figure reproduced with permission from ref.[55], Sage Publications.

requires 3 LEDs (working with different voltages) in the same optical encapsulation. The fore mentioned further reduces packaging costs, size and consumption.

In ref.[58] a comparison study using both technologies concluded the luminous efficacy of a phosphor-white device typically equals more than twice the efficacy of the corresponding RGB combination. The blue LED with *PDMS* : *phosphor* encapsulation unlocked illumination worldwide with a reduced energy consumption, luminous efficiency, durability and more eco-friendly compared with previous illuminating technologies[59].

The solid-state lighting area also includes display devices. The main importance of the *PDMS* : *phosphor* layer in the case of display devices lies in flexible luminescent films and backlight function. The first exploits the flexibility and stretchability of PDMS. The latter exploits the variation of the light emitted by the phosphor, controlling the intensity of the illuminating LED. Despite being a matured technology with good quantum yield while maintaining high thermal and chemical stability, the size of the phosphor particles is in the micron level, increase difficulties in integrating these coatings with micro-LED pixels from displays, affecting color conversion efficiency and uniformity of the devices[60−66].

A green (545 nm) phosphor, $BaLa_2ZnO_5 : Tb^{3+}$, activated with 255 nm light, color purity of 91.03%, quantum efficiency of 49.72% and decay lifetime of 0.520 ms is reported in ref.[47]. The author suggests a *PDMS* : *phosphor* combination for flexible displays use, with chemical stability in environments such as water, but also alkali and acid solutions. Figure 4(a) is a series of photographs of the manufactured films under daylight and UV light, with the latter having a strong PL effect. The author explores the behavior of the films under mechanical stress (Fig. 4(b) and 4(c)) as well as its flexibility (Fig. 4(d)), also suggesting applications in anti-counterfeiting applications and dermatoglyphics, further explained in the next subsections.

Some reported phosphors used for the purpose, as well as metrics related to this subset are listed in Table 3. Correlated color temperature (CCT) is a widely used index to correlate the temperature of an ideal black-body radiator to that of the light source. The color rendering index (CRI) compares the colors in artificial light to the sunlight or standartized light source[67].

Changing the host matrix has influence on the behavior of the phosphor material. For the same powder of phosphor, the reported CCT was 4433 K, 6044 K and 6413 K, for epoxy resin, PDMS and PMMA[43]. A low CRI is related to a deficiency in red light, which usually tends to increase the CCT (higher CCT represents colder light, more close to blue)[78]. Applying the PDMS coating allowed for it to maintain its characteristics over 300 h exposure, contrary to the reference without the encapsulation, which after 120 h had lost nearly 50 percent luminescence[68]. Another common application for *PDMS* : *phosphor* is in head-up displays (HUD), where the transparency of PDMS allows for a transparent display, not interfering with the field of view of the driver, while the phosphor projection displays information for the driver.

Anti-counterfeiting solutions

In this area, the *PDMS* : *phosphor* mixture is mainly used in the form of AC markers, which are invisible in visible light, but are clearly visible when excited by UV radiation. The production of these security tags is low-cost, and using standard screen printing techniques, it is possible to apply them to surfaces such as metal, fabric, paper, and others[38]. These techniques generally imply laying the ink into a hollow patterned screen and subsequent curing of the ink in the material to be marked.

These mixtures are usually prepared with a powdered PDMS mixed with deionized water, where the phosphor is dissolved using ultrasonic baths to ensure uniform dispersion. The solutions are then degassed using vacuum to remove bubbles and cast-dried to form the transparent AC marker, as can be seen in Fig. 5(a). In Fig. 5(b) several printed markers are tested under different environmental conditions, such as different surfaces, long term storage, photo-stability and thermal treatment. Table 4 contains some of the most reported mixtures from the last decades with applications in anti-counterfeiting solutions, using phosphor materials emitting at different wavelengths, combined with PDMS.

A mixture of PDMS and $La_2MoO_6 : Sm^{3+}$ is reported in ref.[38] emitting at 601 nm with excitation light of 365 nm and a quantum yield of 66.2%. In this application characteristics such as chemical and environmental stability are required. These materials must withstand chemical exposures and still ensure durability and reliability. In ref.[57] the stability of the suggested AC marker is demonstrated by evaluating the degradation in different solvents and bleaches such as ethanol, acetone, detergent and hydrogen peroxide The printed security pattern must maintain its phosphorescence during the life cycle

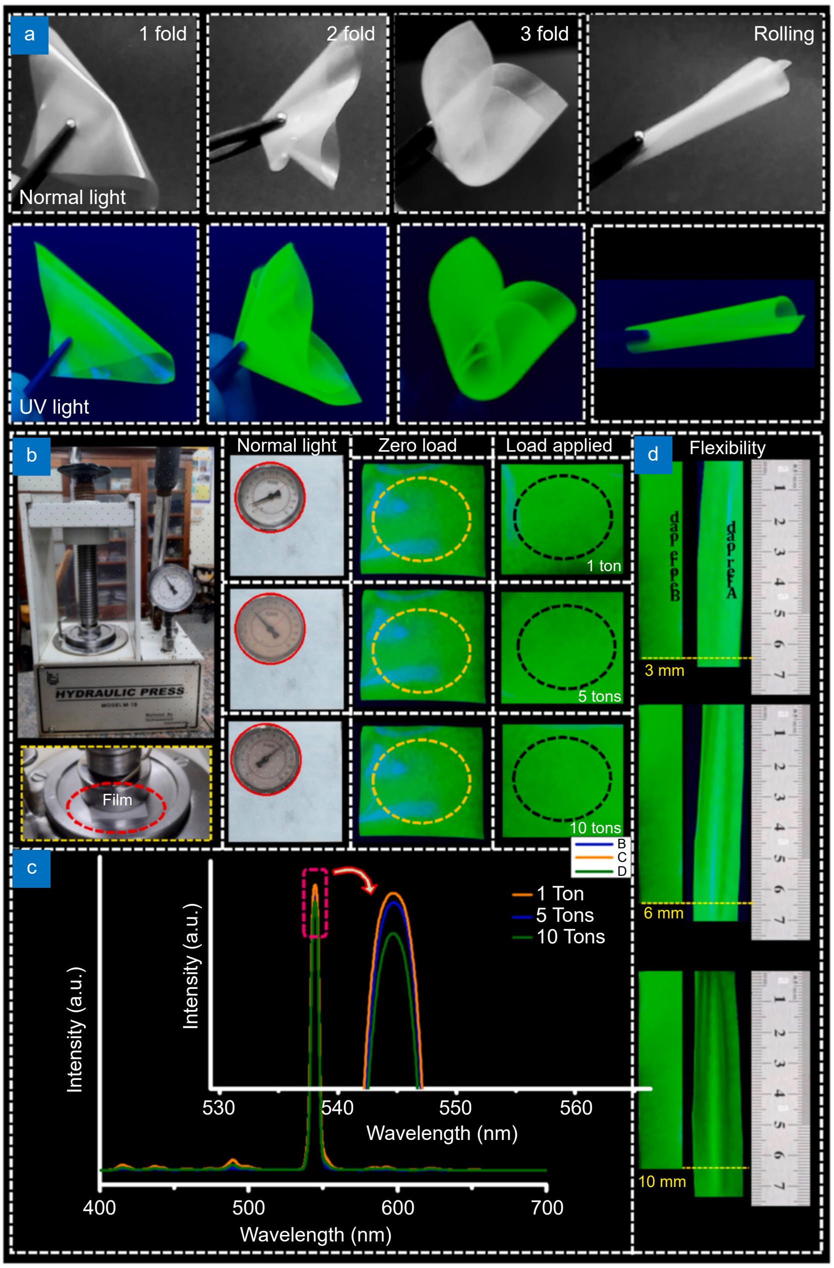

Fig. 4 | (**a**) Photographic images of the $BaLa_2ZnO_5:Tb^{3+}$/PDMS composite folding films under daylight and UV light. (**b**) The $BaLa_2ZnO_5:Tb^{3+}$/PDMS composite film was under applied mechanical stress and photographed before and after applying the mechanical stress under UV 270 nm light. (**c**) PL spectra of films after applying mechanical stress. (**d**) The flexibility of films under different weights (250, 500, and 750 gm). Figure reproduced with permission from ref.[47], Elsevier.

of the object to be protected by the AC marker. The photo-stability must endure prolonged UV exposure and thermal stress. Ensuring all these parameters enables to use these materials as consistent, hard to replicate authentication methods.

Temperature sensors and thermoluminescence

There are many phosphors that exhibit a significant dependence of luminescent behavior on temperature. There are several ways to perform temperature measurements using thermoluminescence, including fluorescence intensity ratio (FIR), luminescence lifetime and emission peak/band width (ref.[23]). Reference[98] reports a green emitting phosphor (550 nm) composed of Y_2O_2S : Er, Yb mixed with PDMS to form a light, flexible thin film thermometer. This very cost-effective device was tested in electronic circuit boards and achieved decimal accuracy for specifically engineered temperature

Table 3 | Phosphors combined with PDMS for white-LED's and solid-state lighting.

Phosphor blend	Excitation λ (nm)	CCT (K)	CRI	Ref
$MgTiO_3:Mn^{4+}+YAG:Ce^{3+}$	blue (445)	4518@0.15 mA	68.5	ref.[17]
$CsPbBr_3+CsPbBr_{0.75}I_{2.25}$	blue (445)	6038		ref.[68]
$Ca_2Y(Nb,Sb)O_6:Mn^{4+}$	UV (291)	5534@30 mA	80.30	ref.[69]
$CYN:Eu^{3+}$	NUV (395)	5583@50 mA	88.30	ref.[70]
$CGN:Eu^{3+}$	NUV (395)	4436@50 mA	85.45	ref.[70]
$CLN:Eu^{3+}$	blue (445)	5485@50 mA	80.03	ref.[70]
$CsPbX_3(X=Cl,Br,I)$	blue (445)	5901–3194		ref.[71]
BODIPY − based organic molecules	blue (445)	4200@150 mA	95	ref.[72]
red and green CdSe/ZnS QDs	UV (291)	6389@50 mA	63.3	ref.[73]
$K_3La(VO_4)_2:Dy^{3+}/Eu^{3+}$	NUV (309)	3813–1713		ref.[74]
$YAG:Ce^{3+}$	blue (470)	4200		ref.[75]
$YAG:Ce^{3+}+CaAlSiN_3:Eu^{2+}$	blue (455)	5000–3000@350 mA	70–80	ref.[76]
$YAG:Ce^{3+}$, $CaS:Eu^{2+}$	blue (445)	3014–4187@500 mA	95.3–92.8	ref.[36]
$CaMoO_4$, $CaMoO_4:Dy^{3+}$	UV (297)	5877		ref.[77]
$Y(OH)_3:Eu^{3+}$	NUV (365)	3900–3600	60	ref.[78]
$SrMoO_4:[Eu^{3+}]/[Tb^{3+}]$	UV (290)	4338		ref.[79]
carbon dots (CDs)	NUV (350)	6649	96	ref.[16]
$Ba_3Lu_4O_9:Bi^{3+},Eu^{3+}$	UV (365)	5870–1834		ref.[80]
YAG:Ce,Gd	blue (455)	6044	82	ref.[43]
red/yellow phosphor	blue (465)	6905–3432	66.26–81.50	ref.[81]
$Sr_{2.765}Gd_{0.09}AlO_4F:0.1Eu^{3+}$	UV (285)	1748	56	ref.[82]
$Sr_{2.795}Y_{0.07}AlO_4F:0.1Eu^{3+}$	UV (285)	1793	54	ref.[82]
$CsPbBr_3$, $CsPbBrI_2$	NUV (375)	6113@15 mA		ref.[83]
red CdSe/ZnS QDs	NUV (400)	5742		ref.[84]
$YAG:Ce^{3+}$	NUV (425)	34002–6905		ref.[85]
$YAG:Ce^{3+}$	blue (450)	6119–5163@200 mA		ref.[86]
$YAG:Ce^{3+}$ + glass beads	blue (455)	6300@0.35 mA	83	ref.[87]
$YAG:Ce^{3+}+Sr_2Si_5N_8:Eu^{2+}$	blue (478)	8000–2900@0.35 mA	82–54	ref.[88]
YAG phosphor	blue	5300–4800@120 mA		ref.[89]
CrO_2 + YAG phosphor	blue (450)	6275–4807@80 mA		ref.[90]
$YAG:Ce^{3+}$	blue OLED	4200		ref.[75]
$YAG:Ce^{3+}$	blue (470)	6700–5666		ref.[41]
$CaWO_4$, $Gd_2(WO_4)_3:Eu^{3+}$	UV (254)	6737–1779		ref.[91]

ranges. The device uses a upconversion mechanism, emitting high-energy photons by fusing low-energy photons[99], as visible in Fig. 6.

Typically in cells or biological tissues, UV excitation may cause interfering luminescence from the surrounding medium, affecting measurements, in contrast to IR excitation, which stimulates visible fluorescence only on the target phosphor[98]. In the case of upconversion phosphors, temperature can be measured using FIR relation with temperature, as in ref.[101] where its use is suggested in silicon chips, where the difference in value for the calibration measurements can be related with the low thermal conductivity of PDMS (0.23 W/mK), especially compared with the silicon chip (167.00 W/mK).

Temperature can also be measured by analysing the decay times of the phosphorescent state. The temperature increase decreases the decay times and the rise time of the emissions as reported in ref.[98]. A *PDMS* : *phosphor* mixture is reported in ref.[26] with thermometry applications and previous reported ± 0.05 °C resolution and target of ± 0.03 °C, using a single layer deposited using spin coating, which can further reduce manufacturing costs

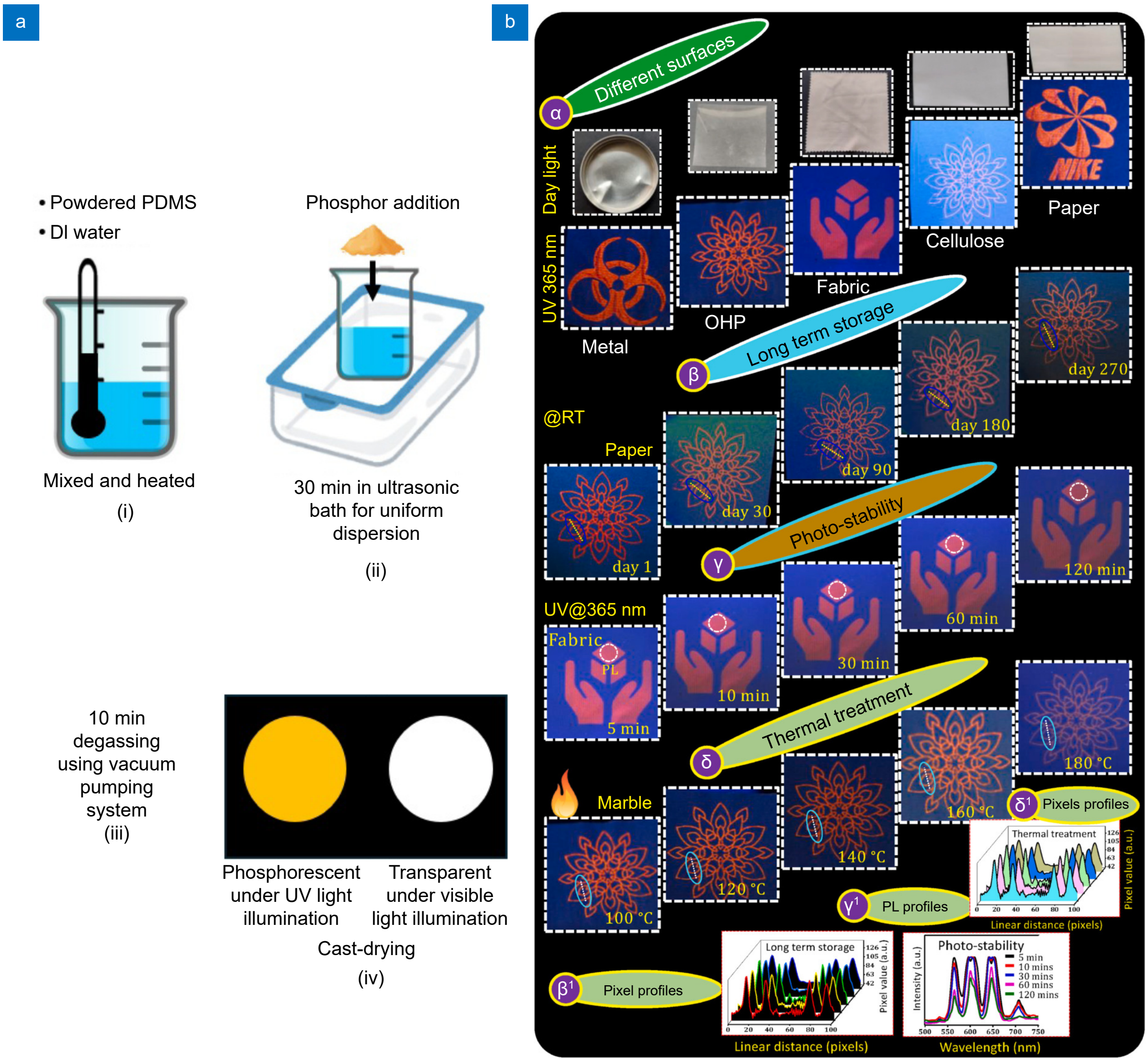

Fig. 5 | (**a**) Diagram of *PDMS*:*phosphor* AC inks manufacturing process. (**b**): (α) AC labels created using screen-printing mode on different surfaces and visualized under day light and UV 365 nm light. (β) Long term storage of AC labels up to 270 days. (γ) Photo-stability test examined up to 120 min using UV source. (δ) Developed AC image on marble and thermally treated up to 250 °C for 20 min (β¹ & δ¹) Pixel profiles of experiments on developed AC labels (γ¹) PL measurement on UV irradiated AC label. Figure reproduced with permission from ref.[38], Elsevier.

Table 4 | Phosphors combined with PDMS for AC solutions.

Phosphor	Ref.	Phosphor	Ref.
$La_2MoO_6:Sm^{3+}$	ref.[38]	$BaGd_2ZnO_5:Ho^{3+}$	ref.[40]
$CaF_2:Er^{3+}$	ref.[19]	$CaAl_{12}O_{19}:Eu^{2+/3+}$	ref.[20]
$BaGd_2ZnO_5:Sm^{3+}$	ref.[92]	$Ba_2LaTaO_6:Mn^{4+}$	ref.[22]
$SrAl_2O_4:Eu^{2+}, Dy^{3+}$	ref.[21]	$Li_8CaLa_2Ta_2O_{13}:Eu^{3+}$	ref.[93]
$CaSrSb_2O_7$, $CaSrSb_2O_7:Bi^{3+}$	ref.[94]	$Sr_2YSbO_6:Eu^{3+}$	ref.[95]
$Ca_{2-x}Nb_2O_7:xPr^{3+}$ $(x=0.00075,\ 0.001,\ 0.002,\ 0.003,\ 0.004)$	ref.[96]	$Ca_2Nb_2O_7:Er^{3+}/Pr^{3+}$, $ZnS:Cu^{2+}$	ref.[97]
$SrAl_2O_4:Tb^{3+}/M$, $(M = Li^+, Na^+, K^+, Ca^{2+}, Bi^{3+})$	ref.[39]		

when optimized. A device achieving repeatability and cyclic temperature measurement with the worst resolution recorded being 0.0011%.K and the best 0.00436%.K (423 K) in the temperature range of 353–523 K is reported in ref.[24], so for short-term it can withstand higher temperatures than the specified by the manufacturer, however is not recommended since it can alter the intrinsic characteristics of PDMS. Table 5 contains some reported mixtures with applications in temperature sensors and thermoluminescence. PDMS Sylgard 184 has a temperature range specified by the manufacturer as −50 °C to 200 °C, limiting its use to this operational range.

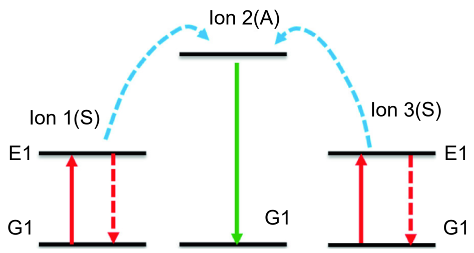

Fig. 6 | Diagram of the upconversion mechanism where the energy absorbed by ion 1 and 3 (E1) is transferred to ion 2 which then emits a photon with higher energy than the ones absorbed when returning to the fundamental state (G1). Figure reproduced with permission from ref.[100], Elsevier.

Bio-medical applications

The mixture of PMDS and phosphor can be a hot topic for biosensors due to several key reasons like enhanced sensitivity (where Phosphor materials can exhibit strong and stable phosphorescence, which can be highly sensitive to changes in the environment. This makes it possible to detect low concentrations of biological targets with high sensitivity; and the combination of PDMS with phosphor can amplify the detection signal, making it easier to detect small changes in the biosensor's environment). Secondly, both PDMS and phosphors are chemically stable materials, which helps in maintaining the integrity and functionality of the biosensor over time as well as these materials can also provide thermal stability, ensuring that the biosensor performs reliably across a range of temperatures. Third point, PDMS is a flexible and stretchable polymer, which can be useful for developing wearable biosensors or sensors that need to conform to irregular surfaces[5]. The PDMS matrix enables a strain sensing in a wide range of strain, spanning up to several hundred percent in comparison to the conventional rigid matrix composites and ceramic-based mechanoluminescence (ML) sensors[106]. It is reported that the mixture of PDMS with ML phosphors is suitable for monitoring of human motions[107]. Mechanoluminescence usually implies applying pressure to a previously excited ion releases a trapped hole to the valence band of the material. This trapped hole can recombine with the ion leading to a unstable state. When returning to a stable state the ion will emit the extra energy in the form of phosphorescent light, which can be correlated with the applied pressure[27,28]. Figure 7(a) illustrates a ML process example.

In this way, such mixture can be used in various types of biosensors, including optical, electrochemical, and mechanical sensors, providing a broad range of applications[108,109]. Not less important is biocompatibility feature: both PDMS and certain phosphor materials are biocompatible, making them safe for use in direct contact with biological tissues and fluids. This biocompatibility ensures that the sensors do not induce adverse biological responses, which is critical for *in vivo* applications. Due to the high elasticity of PDMS (and therefore the PDMS phosphor mixture), at relatively small compressive and tensile forces acting on the PDMS (or the PDMS phosphor mixture), there are negligible changes in the compression or stretching of the PDMS or the PDMS phosphor mixture. Hence, this high elasticity is the main factor for the easy and highly efficient use of mechanoluminescence in the mixture of PDMS and ML phosphor. And this key feature is then easily used in many pressure and tensile biosensors. Customizable properties (by adjusting the ratio of PDMS to phosphor, the mechanical properties of the sensor can be tuned to meet specific requirements, such as elasticity and hardness) and optical tuning, such as emission wavelength and intensity, can be adjusted by choosing different types of phosphors, allowing for the customization of the sensor for specific applications.

Table 5 | Phosphors combined with PDMS for temperature sensors or thermoluminescence.

Phosphor	Ref.	Phosphor	Ref.
$LuNbO_4 : Eu^{3+}/Sm^{3+}$	ref.[24]	La_2O_2S:Eu	ref.[26]
$Ca_2Sb_2O_7 : Eu^{3+}$	ref.[25]	$La_3Ta_{0.8}Sb_0.2O_7 : 0.04Bi^{3+}, zSm^{3+} (0 \leq z \leq 0.03)$	ref.[23]
$SrWO_4 : [Er^{3+}]/[Yb^{3+}]$	ref.[99]	$NaNbO_3 : Pr^{3+}$, hexagonal boron nitride nanosheets	ref.[102]
Y_2O_2S : Er, Yb, La_2O_2S : Yb, Er	ref.[98]	La_2O_2S:Eu	ref.[103]
La_2O_2S:Eu	ref.[104]	$NaGdTi_2O_6 : Pr^{3+}, Er^{3+}$	ref.[105]

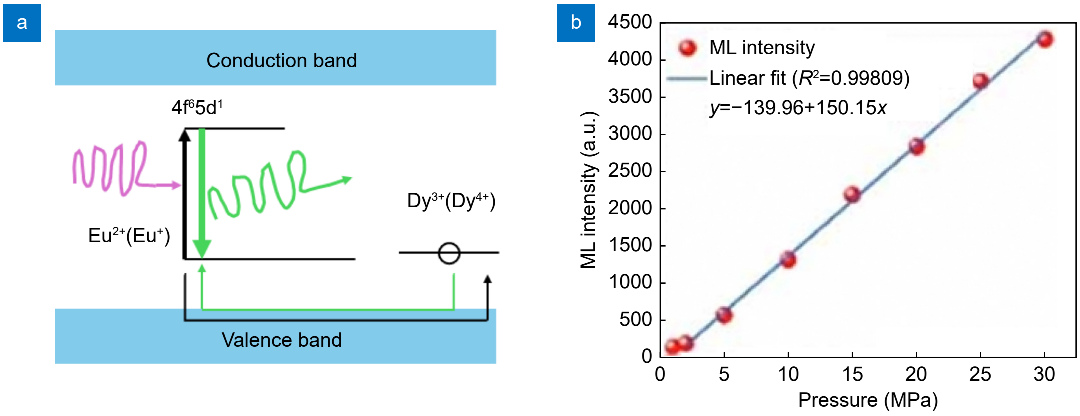

Fig. 7 | The ML properties of the sensor for visual sensing. (**a**) ML mechanism of $SrAl_2O_4{:}Eu^{2+}$, Dy^{3+}. (**b**) The dependence of the ML spectra at varying pressure in the range from 1 MPa to 30 MPa. Figure reproduced with permission from ref.[27], IOP Publishing.

Both PDMS and phosphors are relatively inexpensive materials, which can help in reducing the overall cost of biosensor production. For scalable manufacturing, the fabrication process for PDMS-based biosensors is scalable, allowing for mass production and wider adoption in various fields. Phosphorescent signals typically have longer lifetimes compared to fluorescent signals, which can help in reducing background noise and improving the signal-to-noise ratio in biosensor readings. As last point, PDMS is commonly used in microfluidic devices due to its ease of molding and bonding. Integrating phosphor materials into PDMS can create advanced microfluidic biosensors with enhanced detection capabilities. New bio-medical applications of *PDMS* : *phosphor* blends are being published every year, showcasing that it is a high interest topic both for industrial and academical communities. According to ref.[110] ML also occurs if the device is stretched, allowing its application into tension sensors. A pressure sensor measuring from 1 MPa to 30 MPa using PDMS:$SrAl_2O_4 : Eu^{2+}, Dy^{3+}$ was reported by ref.[27] with ML intensity linear relation with the pressure applied, visible in Fig. 7(b). These devices are bio-compatible and flexible, allowing its application into the human tissues or flexible fabrics[110]. Mechanoluminescence has also been used in Photothermal Therapy, where tumor cells are selectively destroyed without affecting normal tissues, using photothermal agents. These agents usually have persistent luminescent, such as, $ZnGa_2O_4 : Cr^{3+}$ and are activated using mechanoluminescent $SrAl_2O_4 : Eu^{2+}$, remotely actived using ultrasonic waves. A device capable of multicolor fluorescence imaging is reported in ref.[111]. This device uses PDMS light-guide plates to guide the transmitted light from the light source only to the fluorescent samples. PDMS host matrix can be doped with phosphors to enhance the PL intensity of the signal, obtaining higher contrast imaging of the samples. This technology can also be used to monitor in real-time drug releases in specific targets[112]. *PDMS* : *phosphor* based devices can be used to detect tumor biomarkers, metabolites, biomolecules, and other signal parameters from living cells. Luminescent properties of nanoparticles gained notoriety as potential in cell stimulation and tissue growth, providing more efficient tissue engineering strategies[112]. Table 6 comprises several works in ML using different *PDMS* : *phosphor* mixtures.

Other selected applications

One of the possibilities of using the *PDMS* : *phosphor* mixture is in the area of reducing biological pollution in marine infrastructure, heavily affected by bio-foulings. Diatoms, unicellular algae, are known to be one of the major bio-fouling agent. A mixture of PDMS and Waterproof long afterglow phosphors (WLAP) is used to influence the physiological activity of diatoms. WLAP absorbs and stores energy from daylight, which then emits weak fluorescence at night, which limits the physiological activities of diatoms. According to ref.[126], with the use of PDMS and WLAP, attachment reduction rate was 34.5% compared with the blank control sample and a diatom removal rate after wash of 42.3%.

As referred in subsection *White-LED's and display technology*, white emitting LEDs using phosphor coatings is widely used as illumination, however, for certain applications other spectrums are required, such as plants growing. Therefore, the mixture of *PDMS* : *phosphor* can also be engineered to emit in specific wavelengths preferred by the plants. With this approach the efficiency of indoor growing can be further optimized, because all the

Table 6 | Phosphors combined with PDMS for mechanoluminiscence.

Phosphor	Ref.	Phosphor	Ref.
silver nanowire(AgNW), $SrAl_2O_4:Eu^{2+},Dy^{3+}$	ref.[27]	$BaSi_2O_2N_2:Eu^{2+}$	ref.[28,110]
$\beta-KMg(PO_3)_3:Tb^{3+}$	ref.[29]	ZnS : Cu, ZnS : Mn	ref.[35]
$Gd_3Ga_5O_{12}:A(A=Eu^{3+},Tb^{3+},Bi^{3+})$	ref.[30]	ZnS : Mn : Eu	ref.[113]
$ZrO_2:Ti^{4+}$	ref.[114]	$Lu_3Al_5O_{12}:Ce^{3+}$	ref.[115]
$SrZnSO:Bi^{3+}$	ref.[116]	ZnS : Cu	ref.[117,118]
$Ca_2Nb_2O_7:Er^{3+}/Pr^{3+}$, $ZnS:Cu^{2+}$	ref.[97]	$SrAl_2O_4$: Eu,Dy	ref.[119]
$SrAl_2O_4:Eu^{2+},Dy^{3+}$	ref.[120]	$Sr_4Al_{14}O_{25}:Eu^{2+},Dy^{3+}$, ZnS : Cu	ref.[121]
ZnS : Cu	ref.[122]	ZnS : Cu, $Sr_2MgSi_2O_7:Eu^{2+},Dy^{3+}$ dye/$Sr_4Al_{14}O_{25}:Eu^{2+},Dy^{3+}$	ref.[123]
ZnS : Mn	ref.[45]	ZnS : Cu	ref.[124]
ZnS : Al, Cu, ZnS : Al, Cu, Mn	ref.[125]	ZnS : Cu	ref.[44]

light emitted can be in fact the required and absorbed by the plant. A mixture using $Sr_2ScSbO_6:Mn^{4+}$ is reported in ref.[127] with an emitting peak at 697 nm if under 365 nm UV light excitation, matching with the far-red light photosensitive pigment of the plant. According to ref.[128], using 313 nm and 380 nm exciting light in $Rb_xK_{2-x}CaPO_4F:Eu^{2+}(0\leq x\leq 2)$, which emitted in 495 nm and 665 nm, increased the growth rate of Chlorella 12.2% when compared with the control group. Plants require UV and blue wavelengths which can degrade the host material after long exposure, requiring the host matrix to be resistant to these radiation, such as PDMS[129].

The phosphor capabilities can also be harnessed to modulate the emitted light by varying the alternating current frequency applied to the $PDMS:phosphor$ devices and PDMS allows it to have stretchability. According to ref.[130] a device built with PDMS:ZnS:Cu emitted green (0.165, 0.320) with 1 kHz to blue (0.121, 0.131) with 100 kHz. A device where varying the current frequency from 100 Hz to 500 Hz changes the color coordinates from (0.24, 0.42) to (0.23, 0.32) is reported in ref.[131], with ZnS:(Cu, Cl) as phosphor material. In Fig. 8(a) is possible to observe the schematic diagram of the device, AC source and emission.

Another potential application is in Visible Light Communication (VLC), which according to ref.[86] can replace Wi-Fi in the future, being able to combine illumination and communication. A device capable of optical communications is reported in ref.[35], using as information units a multi-color display, activated by pressure on the copper outer layer. The author suggests to use the different emitted colors to code data to be transmitted, as visible

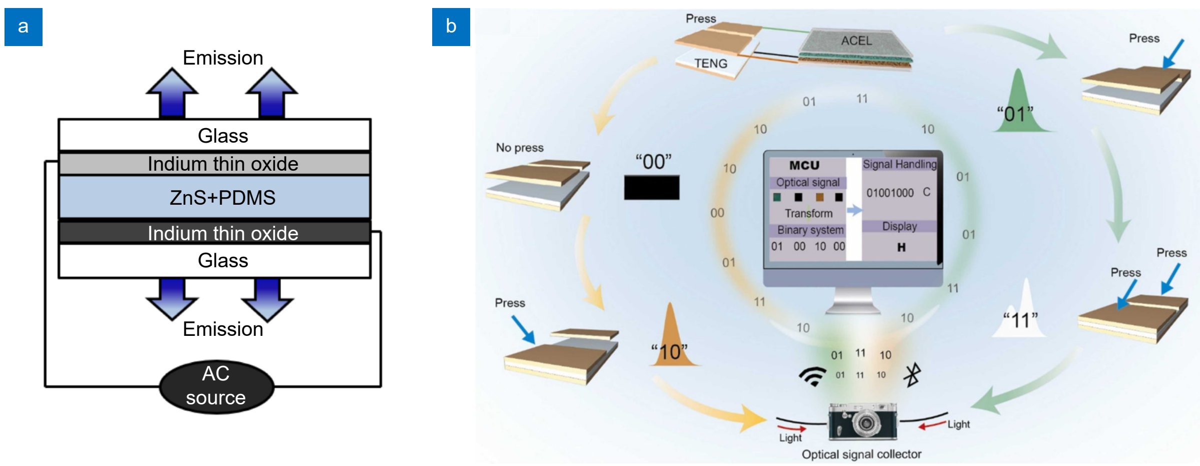

Fig. 8 | (**a**) Schematic of light emission from the mixed ZnS composite and PDMS with applied AC bias. (**b**) Schematic diagram of self-powered optical communication system consisting of information inputs (instantly dynamic self-powered multi-color display), information acquisitions (cameras), information processing (MCU), and information display (display screens). Four information units (00, 01, 10, and 11) and corresponding states of multi-color self-powered ACEL system. Figure reproduced with permission from: (a) ref.[131], under a Creative Commons Attribution Non-Commercial License; (b) ref.[35], Elsevier.

in Fig. 8(b).

However, one issue related with using this technology for communication is the decay time of the phosphor. In optical communication the higher the bit rate and transferred data the higher the frequency at which the light must be modulated. The high decay times of the phosphors limit its available bit rate[132].

Carbon dots have been reported to react with metal ions, altering its luminiscence when excited under UV light and thus with potential use in metal sensing[31]. According to ref.[133] several carbon dots obtained from different biowaste sources are evidenced to have phosphorecent properties, with each interacting in its own manner with the metal ions. The author also suggests this relation to develop metal ion detectors.

X-ray photons are highly energetic and typically are sensed using scintillators and charge-couple device (CCD) sensors. There is a need to use scintillators, which convert the X-ray energy into visible photons, that can be detected by a photodetector, as a CCD sensor or Positive-Intrinsic-Negative (PIN) diode. In this realm, PDSM:phosphor mixtures are of high interest, due to the cost-effective X-ray sensing solution, especially when compared with typicall scintillators made of crystals, such as Cesium Iodide (CsI). Photodetectors for visible light are the most documented and matured, allowing for a high resolution very cost-effective sensing. In this application the higher the resolution possible the better. Resolution is thus a function of the scintillator and the photodetector. A flexible scintillator film made of PDMS:$Ba_2LuNbO_6:Tb^{3+}$ is reported in ref.[134], with a spatial resolution of 12.5 lp/mm, compared with a commercial scintillator in Fig. 9(a).

Fiber optical pH sensors typically use as detection techniques wavelength or amplitude modulation. The first is based on refractive index changes in the sensing layers of the optical fiber, usually having high requirements for the coating and material properties. The latter involves measuring the variation in the output intensity of fluorescent indicators. A sensor manufactured with the mixture PDMS:$NaBaScSi_2O_7:Eu^{2+}$ and, using amplitude modulation, displayed a linear response, visible in Fig. 9(b) and a sensitivity of 0.05/pH in a range of 6.86–9.18 pH[135].

Tryptophan, which is an amino acid, plays an important role in the production of serotonin, melatonin, niacin, and nicotinamide[136]. Tryptophan fluorescence can be used to track cellular proliferation in events such as wounds closure, neoplasm and others chronic conditions with the emission peak located around 345 nm[137]. However, in general, the transmission of optical fibers in this wavelength range is lower. The author suggests using a *PDMS : phosphor* junction converting the peak emission to a 450–650 nm range, improving UV emitters monitoring[137].

Metasurfaces are a new brand of optical engineered materials which use sub-wavelength structures to control the light, as if classical refractive optics, but with the advantage of being flat and thin. To manufacture metasurfaces is thus required to produce structures such as grooves in the nanometer scale. A combination of PDMS:phosphor is suggested in ref.[33] for a metasurface engineered flexible sticker with luminescent characteristics. These films can found applications in photovoltaic panels. The upconversion mechanism overviewed in section *Temperature sensors and thermoluminescence* as po-

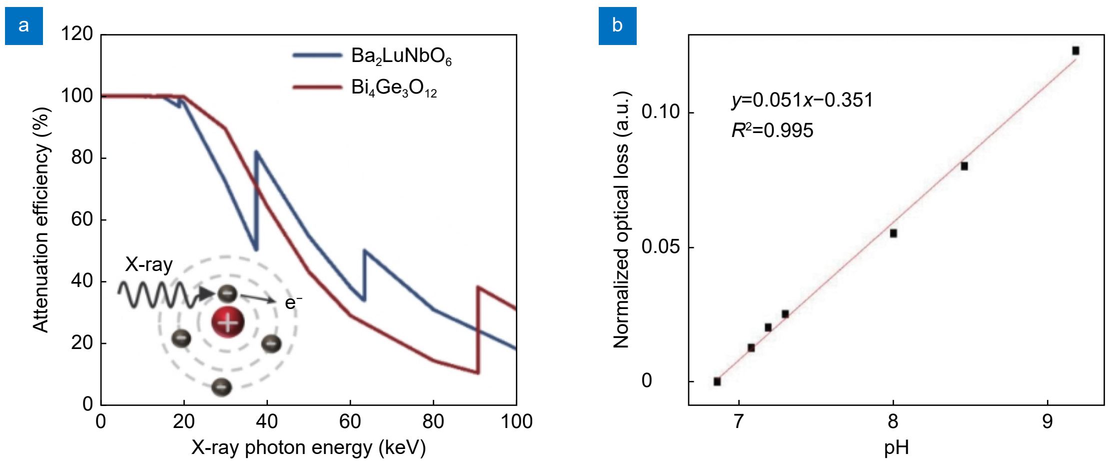

Fig. 9 | (**a**) X-ray energy absorption spectra of $Ba_2LuNbO_6:Tb^{3+}$ and the commercial scintillator $Bi_4Ge_3O_{12}$. (**b**) Normalized optical loss relation with pH. Figure reproduced with permission from: (a) ref.[134] and (b) ref.[135], respectively.

tential uses in photovoltaic applications. Commercial photovoltaic panels are manufactured using silicon, which has lower absorption in the low-energy end of the visible spectrum, with trace amounts of IR photons being absorbed. In a way to increase efficiency of photovoltaic panels, ref.[138] suggests coating the panels with PDMS: β-$NaYF_4$:Yb^{3+}/Er^{3+}, a phosphor with peak emission at 543.5 nm.

Another suggested application is a robust and cost-effective sensor for analytes, such as dissolved CO_2, with its scheme visible in Fig. 10(a)[34]. This device uses a phase-based sensing technique, luminophore referencing (DLR) using a film of PDMS:Ru(dpp)$_3^{2+}$ used as reference luminophore and other fluorescent indicator, achieving a R^2 = 0.993, as visible in Fig. 10(b). Combining bio-compatibility and dissolved gas detection allows for real time monitoring in tissues, cell cultures or water as reported in ref.[139], achieving a low limit of detection of 0.01 mg/L, a high sensitivity of 16.9 and a short response time (22 s).

An application in heat flux sensing is suggested in ref.[98]. The PDMS:Y_2O_2S:Er,Yb mixture can be introduced in fluids, with the phosphor embedded into the PDMS matrix to form small sensing clusters, and using thermoluminescence, previous referred in section *Temperature sensors and thermoluminescence* is thus possible to map the heat flux along liquid solutions. Pressure-sensitive paints, used in the aerospace industry for aerodynamic studies of the aircraft are of great interest. A matrix of PDMS with Tetra (pentafluorophenyl)porphine (PtTFPP) was reported by ref.[140] to have a short response time and very low photo-degradation rate. Using the remote optical sensing capabilities of *PDMS* : *phosphor* films[33] suggests using them as non-destructive, remote, instantaneous, and customizable sensors to identify geometrical defects in aerogels and elastomers, materials that serve as critical structural components while operating in extreme conditions, such as PDMS. Another well investigated use of these misture is in dermatoglyphics studies. Dermatoglyphics is the scientific study of indicators in the skin such as fingerprints. Using these materials can enhance the ability to distinguish patterns and to improve imaging qualities[47]. Table 7 summarizes some of the several uses where a blend of *PDMS* : *phosphor* was applied.

Discussion and future perspectives

The *PDMS* : *phosphor* mixture has many advantages, with a symbiotic relationship existing and bringing several advantages. The optical tunability in all the visible spectrum that engineered phosphorescent materials hosted in a PDMS matrix offers is of high interest in many industries. It is a core technology for cleaner energetic transition in illumination and displays solutions worldwide and will continue to further help, for instance in food production, with higher efficiency indoor growing systems. PDMS is a well known bio-compatible material, and this characteristic as well as its polymeric structure giving it a elastic and stretchable form, allows for several bio-medical applications, such as sensors or bio-imaging. Another well documented advantage of using *PDMS* : *phosphor* based solutions is the easy manufacturing with high repeatability and cost-effective solutions. Some of these characteristics in phosphor materi-

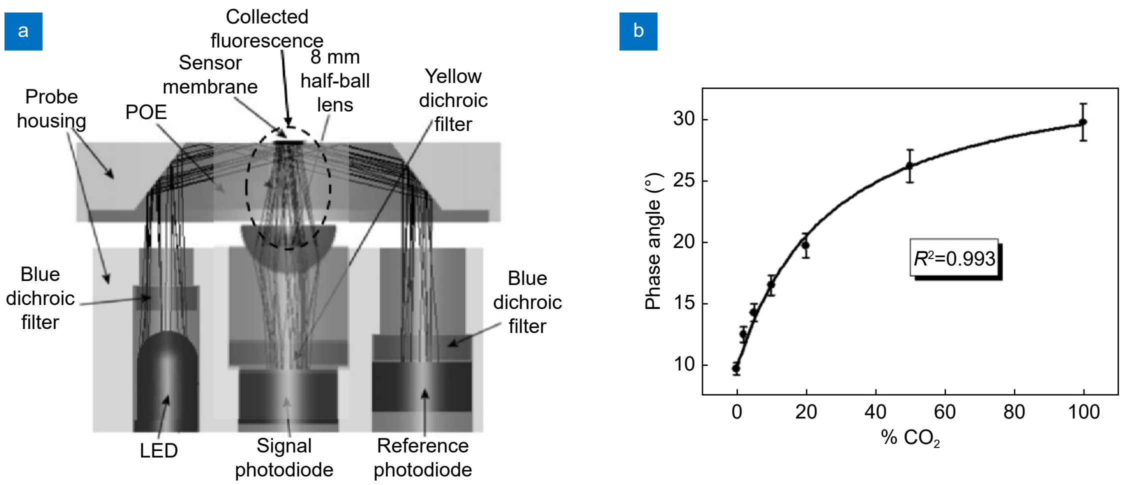

Fig. 10 | (**a**) Schematic of sensor probe excitation configuration and collection scheme. (**b**) Calibration curve of PDMS-based CO_2 sensor. Figure reproduced with permission from ref.[34], Elsevier.

Table 7 | Phosphors combined with PDMS for uses in various applications.

Area of application	Phosphor	Ref.
Biological antifouling	$Sr_2MgSi_2O_7:(Eu^{2+}, Dy^{3+})$, Waterproof Long Afterglow Phosphors (WLAP), Blue-Green (BG), Yellow-Green (YG), Sky Blue (SB) LAP	ref.[126,141–144]
Color change due to Biased AC electric field	ZnS:(Cu, Al, Mn), Tetrapod-Like ZnO Whiskers, ZnS:(Cu, Cl)	ref.[131,130]
Visible Light Communication (VLC)	ZnS:Cu, ZnS:Mn, YAG:Ce, CaS:Eu, Red and Green CdSe/ZnS QDs, YAG:Ce	ref.[35–37,73,86,132]
Plant growth LEDs	Sr2ScSbO6:Mn^{4+}/Li^{+}, $Rb_xK_{2-x}CaPO_4F:Eu^{2+}$($0 \le x \le 2$), $Sr_9Ca(Li, Na, K)(PO_4)_7:Eu^{2+}$	ref.[127,128,145]
Heavy metal ions detection	Carbon Dots (CD)	ref.[31]
X-ray detection, imaging, X-ray information storage	$Ba_2LuNbO_6:Tb^{3+}$, Gd_2O_2S:Tb, 2,5-Diphenyloxazole (PPO), 1,4-Bis(5-Phenyloxazol-2-yl)Benzene (POPOP), La_2O_2S:Eu	ref.[134,146–148]
pH sensor	$NaBaScSi_2O_7:Eu^{2+}$, $BaMoO_4:Eu^{3+}$, CePO4:Tb^{3+}	ref.[32,149]
Optical fiber fluorosensor	Eu-Activated Phosphors	ref.[137]
LED color filter	$SrWO_4$:[Sm^{3+}/Dy^{3+}], $CaMoO_4$, $CaMoO_4:Dy^{3+}$, $BaMoO_4$:[Sm^{3+}/Dy^{3+}], $SrMoO_4$:[Eu^{3+}/Tb^{3+}]	ref.[150,77,151,79]
Metasurfaces	Silicon Nanoparticles	ref.[152]
Detection of geometric defects in materials	La_2O_2S:Eu, Mg3F_2GeO_4	ref.[33]
Solar cells	$(Ba, Sr)_2SiO_4:Eu^{2+}$, β-$NaYF_4:Yb^{3+}/Er^{3+}$ or Ho^{3+} or Tm^{3+}, β-$NaYF_4:Yb^{3+}/Er^{3+}$	ref.[153,154,138]
Oxygen sensor	$Ru(dpp)_3Cl_2$	ref.[155]
Detection of dissolved carbon dioxide	$Ru(dpp)_3^{2+}$	ref.[34]
Pressure-sensitive paint	Platinum Tetra(pentafluorophenyl)porphine (PtTFPP)	ref.[140]
Dermatoglyphics	$BaLa_2ZnO_5:Tb^{3+}$, $SrAl_2O_4:Tb^{3+}/M$, ($M = Li^{+}, Na^{+}, K^{+}, Ca^{2+}, Bi^{3+}$)	ref.[47,39]
Heat flux sensor	Y_2O_2S : Er, Yb, La_2O_2S : Yb,Er	ref.[98]

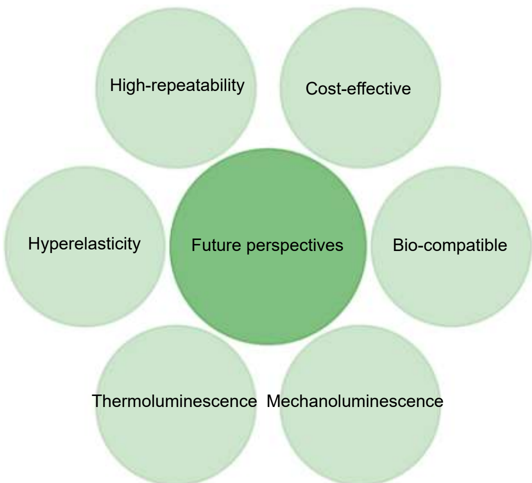

Fig. 11 | Capabilities of the *PDMS:phosphor* mixture for future perspectives applications.

als are summarized in Fig. 11.

However, despite all the advantages of these blends, there are certain issues to be solved, such as optical quenching. As referred before, PDMS has a low thermal conductivity, which can affect the measurements if used in thermometry applications but also affects its ability to disperse heat. This creates others problems also referred such as temperature quenching, that with time reduce the PL intensity. The luminance and efficiency of the phosphor over time is reduced due to poor thermal management causing crackings in the interface between the host and the phosphor[55]. Its temperature range can also be a limiting factor for the mixture if the application requires temperatures lower than −50 °C and higher than 200 °C, or a use of a specifically tuned PDMS, since most commercial available PDMS only withstand the referred temperature. The mechanical properties of PDMS are changed after introducing the phosphor, which may lead to increased brittleness or reduced flexibility. Using PMDS:phosphor blends requires a trade-off between mechanical robustness, and thus durability, and optical efficiency, which needs to be engineered for the specific application. If there is a phase separation or uneven distribution between the PDMS and the phosphor the luminescence will be non-uniform and the performance will be reduced. This however, is a feature that can be exploited for new anti-counterfeiting solutions.

On the other hand, it is very likely that many new applications will be discovered in some areas, especially in the field of mechanoluminescence where new bio-medical applications are reported frequently. Combining mechanoluminescence with piezoelectricity on a device using PDMS as host, as reported in ref.[118], provides a comprehensive understanding of mechanical events, providing qualitative and quantitative information about strain-related issues and use artificial intelligence (AI) to further optimize the device. PDMS alone has been reported to be used to manufacture bioinspired multifunctional flexible optical sensor achieving sub-millimeter spatial resolution for force location sensing, plus a μN resolution in force assessment[156]. Electronic skin, wearable electronic sensors mimicking the functionalities of the human skin, manufactured using PDMS have been reported by ref.[157]. These new bioinspired sensors can leverage 3D printing techniques and AI to manufacture complex structures and mixed phosphors can help to boost the collected signal or to retrieve information about the health of the sensor. Here AI will speed the development of sensor technology due to the complex correlations and high-throughput of data in the biomedical contexts, as p.e. in ref.[2], where AI is used to distinguish between signals produced by different pressure and movements in mechanoluminescence devices. In some areas, the $PDMS : phosphor$ mixture has so far been little used, e.g. in the area of VLC. Perhaps the challenge could be to find a better use of the $PDMS : phosphor$ mixture for this area as well, using different phosphor with different energy levels to be able to expand the available range. In photovoltaics area new explored solutions can increase the efficiency of new devices, as well as being able to increase its longevity, with easy to manufacture PDMS films.

Conclusion

In this comprehensive review, all known applications of the $PDMS : phosphor$ mixture over the last decade have been presented. Overviews of phosphors used for individual applications were also presented here, as well as some advantages, disadvantages and trade-offs of using these blends. We believe that this detailed breakdown of phosphors can be very useful for further research work related to the use of the $PDMS : phosphor$ mixture.

To conclude, the combination of PDMS with phosphorescent materials is developing and booming due to its unique optical and mechanical properties while being easy to manufacture and cost-effective. Its versatility and ability to combine with other technologies is a core advantage. Despite having some issues to be solved it is a standard in a wide range of industries from biomedical to illumination, with significant potential applications to be discovered using new processing techniques and innovative material design, while managing trade-offs for each particular application.

References

1. Schneider F, Fellner T, Wilde J et al. Mechanical properties of silicones for mems. *J Micromech Microeng* **18**, 065008 (2008).
2. Ariati R, Sales F, Souza A et al. Polydimethylsiloxane composites characterization and its applications: a review. *Polymers* **13**, 4258 (2021).
3. Carey JA, Collins III WD, Posselt JL. High stability optical encapsulation and packaging for light-emitting diodes in the green, blue, and near UV range, U. S. Patent 6204523B1, March 2001.
4. Li Y, Tao P, Siegel RW et al. Multifunctional silicone nanocomposites for advanced LED encapsulation. *MRS Online Proc Libr* **1547**, 161–166 (2013).
5. Miranda I, Souza A, Sousa P et al. Properties and applications of PDMS for biomedical engineering: a review. *J Funct Biomater* **13**, 2 (2022).
6. Yang LY, Li YP, Fang F, Li LY, Yan ZJ et al. Highly sensitive and miniature microfiber-based ultrasound sensor for photoacoustic tomography. *Opto-Electron Adv* **5**, 200076 (2022).
7. Ko KY, Her EJ, Nichols WT et al. Fabrication of 2D photonic crystal assisted Y2O3: Eu3+ thin-film phosphors by direct nano-imprinting. *Microelectron Eng* **88**, 2930–2933 (2011).
8. Zhang B, Wang JW, Hao LY et al. Highly stable red-emitting $Sr_2Si_5N_8$: Eu^{2+} phosphor with a hydrophobic surface. *J Am Ceram Soc* **100**, 257–264 (2017).
9. Zhang B, Zhang JW, Zhong H et al. Enhancement of the stability of green-emitting Ba_2SiO_4: Eu^{2+} phosphor by hydrophobic modification. *Mater Res Bull* **92**, 46–51 (2017).
10. Yang MT, Cheng S, Yang F et al. Aqueous synthesis of stable Zn alloyed manganese halides for efficient backlit display. *J Lumin* **253**, 119470 (2023).
11. Cai JH, Chen XG, Zhang WY et al. Two-step performance optimization of CsPbBr3 perovskite nanocrystals for wide color gamut displays. *Photonics* **10**, 1113 (2023).
12. Tian M, Wang J, Wang L et al. Blue-emitting orthosilicate phosphor Ba2SiO4: Eu2+ for near ultraviolet excited white light-emitting diodes with high color rendering index. *J Alloys Compd* **895**, 162420 (2022).
13. Li X, Gao P, Wang J et al. Facile synthesis and luminescence properties of Sr3Al2O6Cl2: Eu2+ for security and display applications. *J Mater Sci Mater Electron* **33**, 7708–7715 (2022).
14. Yuce H, Guner T, Balci S et al. Phosphor-based white LED by various glassy particles: control over luminous efficiency. *Opt Lett* **44**, 479–482 (2019).
15. Patnam H, Hussain SK, Yu JS. Luminescence properties of Tb3+/Eu3+ ions activated LiLaSiO4 phosphors for solid-state lighting and flexible display applications. *J Lumin* **263**, 120063 (2023).
16. Perikala M, Bhardwaj A. Excellent color rendering index single system white light emitting carbon dots for next generation

lighting devices. *Sci Rep* **11**, 11594 (2021).

17. Wathook B, Hassan DA, Pang S et al. Phase transformation and photoluminescence properties of MgTiO3: Mn4+ synthesis by modified sol–gel method. *Chem Afr* **7**, 1639–1648 (2024).
18. Jung JJ, Park JJ, Yang HK. White light-emitting calcium tungstate microspheres synthesized via co-precipitation at room temperature and application to UV-LED chip. *J Alloys Compd* **969**, 172353 (2023).
19. Liu HZ, Zhu XY, Nie L et al. Multimode-responsive luminescence of Er3+ single-activated CaF2 phosphor for advanced information encryption. *Inorg Chem* **62**, 16485–16492 (2023).
20. Jiang XP, Guo Y, Wang LX et al. Self-reduction induced CaAl12O19: $Eu^{2+/3+}$: a phosphor with dynamic photoluminescence and photochromism for advanced anti-counterfeiting and encryption. *Ceram Int* **49**, 28729–28740 (2023).
21. Gao P, Wang JG, Wu J et al. Preparation of SrAl2O4: Eu2+, Dy3+ powder by combustion method and application in anti-counterfeiting. *Coatings* **13**, 808 (2023).
22. Hua Y, Yu JS. An anti-counterfeiting strategy of polydimethylsiloxane flexible light-emitting films based on non-rare-earth Mn^{4+}-activated Ba_2LaTaO_6 phosphors. *Mater Today Chem* **26**, 101109 (2022).
23. Xue Y, Chen YQ, Mao QN et al. Energy transfer in Bi^{3+}-Sm^{3+} co-doped phosphors for temperature sensing and imaging. *Mater Des* **234**, 112375 (2023).
24. Chen YQ, Xue Y, Mao QN et al. Tunable luminescence in Eu3+/Sm3+ single-doped LuNbO4 for optical thermometry and anti-counterfeiting. *J Mater Chem C* **11**, 9974–9983 (2023).
25. Shi XY, Xue Y, Mao QN et al. Eu3+ single-doped phosphor with antithermal quenching behavior and multicolor-tunable properties for luminescence thermometry. *Inorg Chem* **62**, 893–903 (2023).
26. Parajuli P, Allison SW, Sabri F. Spincoat-fabricated multilayer PDMS-phosphor composites for thermometry. *Meas Sci Technol* **28**, 065101 (2017).
27. Li N, Sun JL, Chang SL et al. Ultra-wide range tri-mode flexible pressure sensor. *J Phys D Appl Phys* **56**, 345102 (2023).
28. Song H, Zhang ZY, Zhang YJ et al. Occlusal splint with mechanoluminescence properties based on BaSi2O2N2: Eu2+ cyan phosphor prepared by deposition-precipitation method. *J Lumin* **260**, 119876 (2023).
29. Chen HM, Wang L, Zhang P et al. Investigation on photoluminescence and mechanoluminescence of single Tb3+-doped intense green phosphor. *Acta Chim Sin* **81**, 771–776 (2023).
30. Wathook BA, Hassan DA, Pang S et al. Design of phase transition and improved photoluminescence properties in SrTiO3: Mn4+ using a sol–gel combustion method. *J Mater Sci Mater Electron* **34**, 15673–15684 (2023).
31. Guan XL, Li HJ, Yu ZY et al. High-performance $La_{0.75}K_{0.25}MnO_3$: $x$$Ag_2O$ composites based on electron-lattice and electron-magnetic coupling mechanism. *J Alloys Compd* **895**, 162555 (2022).
32. Zhao XQ, Sun XH, Guo RS et al. Bifunctional tin modified SnO_2 nanospheres embedded biomass-derived carbon network for polysulfides adsorption-conversion in lithium-sulfur batteries. *J Alloys Compd* **895**, 162578 (2022).
33. Mitchell KE, Aryal M, Allison S et al. Remote optical detection of geometrical defects in aerogels and elastomers using phosphor thermometry. *Opt Mater* **119**, 111378 (2021).
34. Burke CS, Markey A, Nooney RI et al. Development of an optical sensor probe for the detection of dissolved carbon dioxide. *Sens Actuators B Chem* **119**, 288–294 (2006).
35. Liao J, Sun JL, Dong FY et al. Self-powered, flexible, and instantly dynamic multi-color electroluminescence device with bi-emissive layers for optical communication. *Nano Energy* **112**, 108488 (2023).
36. Jargus J, Tomis M, Baros J et al. Measurement of the effect of luminescent layer parameters on light and communication properties. *IEEE Trans Instrum Meas* **72**, 5500316 (2022).
37. Jargus J, Vitasek J, Nedoma J et al. Effect of selected luminescent layers on CCT, CRI, and response times. *Materials* **12**, 2095 (2019).
38. Krushna BRR, Sharma SC, Prasad BD et al. Fabrication of highly flexible luminescent films, hydro gels and anti-counterfeiting applications of La2MoO6: Sm3+ phosphors. *J Sci Adv Mater Devices* **9**, 100641 (2024).
39. Mamatha GR, Radha Krushna BR, Malleshappa J et al. Investigating the influence of mono-, di-, and trivalent co-dopants (Li+, Na+, K+, Ca2+, Bi3+) on the photoluminescent properties and their prospective role in data security applications for SrAl2O4: Tb3+ nanophosphors synthesized via an eco-friendly combustion method. *Mater Sci Eng B* **299**, 117008 (2024).
40. Girisha HR, Daruka Prasad B, Radha Krushna BR et al. Versatile properties of BaGd2ZnO5: Ho3+ nanomaterial: compatible towards solid state lightening, anti-counterfeiting and biomedical applications. *Inorg Chem Commun* **159**, 111711 (2024).
41. Chen LC, Lin W W, Chen JW. Fabrication of GaN-based white light-emitting diodes on yttrium aluminum garnet-polydimethylsiloxane flexible substrates. *Adv Mater Sci Eng* **2015**, 537163 (2015).
42. Havlák L, Bárta J, Buryi M et al. Eu2+ stabilization in YAG structure: optical and electron paramagnetic resonance study. *J Phys Chem C* **120**, 21751–21761 (2016).
43. Ţucureanu V, Matei A, Avram A. The effect of the polymeric matrix on the emission properties of YAG-based phosphors. *J Alloys Compd* **844**, 156136 (2020).
44. Li JY, Zhang ZW, Luo XX et al. Triboelectric leakage-field-induced electroluminescence based on ZnS: Cu. *ACS Appl Mater Interfaces* **14**, 4775–4782 (2022).
45. Fontenot RS, Allison SW, Lynch KJ et al. Mechanical, spectral, and luminescence properties of ZnS: Mn DOPED PDMS. *J Lumin* **170**, 194–199 (2016).
46. Ma L, Amador E, Belev GS et al. Tuning Ag^{+} and Mn^{2+} doping in ZnS: Ag, Mn embedded polymers for flexible white light emitting films. *Soft Sci* **4**, 1 (2024).
47. Girisha HR, Radha Krushna BR, Manjunatha K et al. Optimized Tb^{3+}-activated highly efficient green-emanating $BaLa_2ZnO_5$ nanophosphors in PDMS matrix for flexible display, anti-counterfeiting, and dermatoglyphics applications. *Mater Today Sustain* **24**, 100493 (2023).
48. Ayoub I, Kumar V. Synthesis, photoluminescence, Judd–Ofelt analysis, and thermal stability studies of Dy^{3+}-doped $BaLa_2ZnO_5$ phosphors for solid-state lighting applications.

RSC Adv **13**, 13423–13437 (2023).

49. Ayoub I, Mushtaq U, Yagoub MYA et al. Structural, optical and photoluminescence properties of $BaLa_2ZnO_5$: Eu^{3+} phosphor: a prospective red-emitting phosphor for led applications. *Opt Mater* **148**, 114797 (2024).
50. Yen WM, Shionoya S, Yamamoto H. *Phosphor Handbook* 2nd ed (CRC Press, Boca Raton, 2007).
51. Wako AH, Dejene FB, Swart HC. Effect of Ga^{3+} and Gd^{3+} ions substitution on the structural and optical properties of Ce^{3+} -doped yttrium aluminium garnet phosphor nanopowders. *Luminescence* **31**, 1313–1320 (2016).
52. Pan YX, Wang W, Liu GX et al. Correlation between structure variation and luminescence red shift in YAG: Ce. *J Alloys Compd* **488**, 638–642 (2009).
53. DOW. SYLGARD™184 Silicone Elastomer Technical Data Sheet. Form No. 11-3184-01-0224 S2D, Accessed: 2024-07-25.
54. Jia J, Zhang AQ, Li DX et al. Preparation and properties of the flexible remote phosphor film for blue chip-based white LED. *Mater Des* **102**, 8–13 (2016).
55. Yazdan Mehr M, Bahrami A, Van Driel WD et al. Degradation of optical materials in solid-state lighting systems. *Int Mater Rev* **65**, 102–128 (2020).
56. Ray S, Tadge P, Dutta S et al. Synthesis, luminescence and application of BaKYSi2O7: Eu2+: a new blue-emitting phosphor for near-UV white-light LED. *Ceram Int* **44**, 8334–8343 (2018).
57. Zhang CN, Uchikoshi T, Takeda T et al. Research progress on surface modifications for phosphors used in light-emitting diodes (LEDs). *Phys Chem Chem Phys* **25**, 24214–24233 (2023).
58. Keppens A, Acuña P, Chen HT et al. Efficiency evaluation of phosphor-white high-power light-emitting diodes. *J Light Visual Environ* **35**, 199–206 (2011).
59. Nair GB, Swart HC, Dhoble SJ. A review on the advancements in phosphor-converted light emitting diodes (pc-LEDs): Phosphor synthesis, device fabrication and characterization. *Prog Mater Sci* **109**, 100622 (2020).
60. Wu YF, Ma JS, Su P et al. Full-color realization of micro-LED displays. *Nanomaterials (Basel)* **10**, 2482 (2020).
61. Lu XL, Cheng DM, Dong FY et al. Tailoring the emission of Eu based hybrid materials for light-emitting diodes application. *J Lumin* **200**, 274–279 (2018).
62. Xu ZH, Xia ZG, Liu QL. Two-step synthesis and surface modification of CaZnOS: Mn^{2+} phosphors and the fabrication of a luminescent poly(dimethylsiloxane) film. *Inorg Chem* **57**, 1670–1675 (2018).
63. Jia J, Jia HS, Zhang AQ et al. Highly elastic and flexible phosphor film for flexible LED lighting and display applications. *Chin J Lumin* **38**, 1493–1502 (2017).
64. Novák M, Fajkus M, Jargus J et al. Analyzing of chromaticity temperature of novel bulb composed of PDMS and phosphor. *Proc SPIE* **10440**, 104400D (2017).
65. Lin HY, Tu ZY, Ku PC et al. Large area lighting applications with organic dye embedded flexible film. *Proc SPIE* **9383**, 93830N (2015).
66. Chawla S, Roy T, Majumder K et al. Red enhanced YAG: Ce, Pr nanophosphor for white LEDs. *J Expl Nanosci* **9**, 776–784 (2014).
67. Choudhury AKR. 1 - Characteristics of light sources. In Choudhury AKR. *Principles of Colour and Appearance Measurement* 1–52 (Elsevier, Amsterdam, 2014).
68. Jang JW, Kim EY, Kwon OH et al. Polymer-encapsulated UV-curable stacked prismatic layers of all-halide phosphor composites for white luminescence. *Mater Des* **224**, 111307 (2022).
69. Hua YB, Xue JP, Yu JS. Design of a novel WLED structure based on the non-rare-earth $Ca_2Y(Nb, Sb)O_6$: Mn^{4+} materials. *Ceram Int* **47**, 24296–24305 (2021).
70. Hua YB, Ran WG, Yu JS. Advantageous occupation of europium(III) in the B site of double-perovskite $Ca_2BB'O_6$ (B = Y, Gd, La; B' = Sb, Nb) frameworks for white-light-emitting diodes. *ACS Sustain Chem Eng* **9**, 7960–7972 (2021).
71. Wang YM, Guo SS, Yan XL et al. Flexible, ultra-stable and color tunable fluorescent films based on all inorganic perovskite quantum dots embedded in polymer. *Nanotechnology* **31**, 345706 (2020).
72. Yuce H, Guner T, Dartar S et al. BODIPY-based organic color conversion layers for WLEDs. *Dyes Pigm* **173**, 107932 (2020).
73. Wang WC, Wang HY, Chen TY et al. CdSe/ZnS core-shell quantum dot assisted color conversion of violet laser diode for white lighting communication. *Nanophotonics* **8**, 2189–2201 (2019).
74. Hussain SK, Go HS, Han JJ et al. Energy transfer mechanism and tunable emissions from $K_3La(VO_4)2$: Dy^{3+}/Eu^{3+} phosphors and soft-PDMS-based composite films for multifunctional applications. *J Alloys Compd* **805**, 1271–1281 (2019).
75. Chen CC, Lin HY, Li CH et al. Enabling lambertian-like warm white organic light-emitting diodes with a yellow phosphor embedded flexible film. *Int J Photoenergy* **2014**, 851371 (2014).
76. Sher CW, Chen KJ, Lin CC et al. Large-area, uniform white light LED source on a flexible substrate. *Opt Express* **23**, A1167–A1178 (2015).
77. Jung JY. White luminescent calcium molybdate phosphor synthesized at room temperature via the co-precipitation method used in a LED flexible composite. *Opt Mater* **132**, 112830 (2022).
78. Guner T, Kus A, Ozcan M et al. Green fabrication of lanthanide-doped hydroxide-based phosphors: $Y(OH)_3$: Eu^{3+} nanoparticles for white light generation. *Beilstein J Nanotechnol* **10**, 1200–1210 (2019).
79. Jung JY. Luminescent color-adjustable europium and terbium co-doped strontium molybdate phosphors synthesized at room temperature applied to flexible composite for LED filter. *Crystals* **12**, 552 (2022).
80. Wang ZY, Chen J, Liu YG et al. Enhanced photoluminescence and energy transfer behavior in $Ba_3Lu_4O_9$: Bi^{3+}, Eu^{3+} for flexible lighting applications. *Spectrochim Acta A Mol Biomol Spectrosc y* **258**, 119829 (2021).
81. Su ZP, Zhao B, Gong Z et al. Color-tunable white LEDs with single chip realized through phosphor pattern and thermal-modulating optical film. *Micromachines* **12**, 421 (2021).
82. Sreevalsa S, Ranjith P, Ahmad S et al. Host sensitized photoluminescence in $Sr_{2.9-3x/2}Ln_xAlO_4F$: $0.1Eu^{3+}$ (Ln = Gd, Y) for

innovative flexible lighting applications. *Ceram Int* **46**, 21448–21460 (2020).
83. Wu ZH, Wang P, Wu J et al. Ultra-stable phosphor of h-BN white graphene-loaded all-inorganic perovskite nanocrystals for white LEDs. *J Lumin* **219**, 116941 (2020).
84. Li ZT, Tang XT, Li M et al. Micro-dimple/pillar array molded by a track-etching mold for improving the optical performance of quantum dot film. In *2019 20th International Conference on Electronic Packaging Technology* (*ICEPT*) 1–4 (IEEE, 2019); http://doi.org/10.1109/ICEPT47577.2019.245161.
85. Jargus J, Nedoma J, Fajkus M et al. The influence of the variable excitation wavelength on the spectral characteristics of the light generated by the luminescent layer consisting of YAG: Ce phosphor and PDMS. *Int J Mech Eng Rob Res* **8**, 361–367 (2019).
86. Vitasek J, Jargus J, Stratil T et al. Illumination and communication characteristics of white light created by laser excitation of YAG: Ce phosphor powders. *Opt Mater* **83**, 131–137 (2018).
87. Güner T, Şentürk U, Demir MM. Optical enhancement of phosphor-converted wLEDs using glass beads. *Opt Mater* **72**, 769–774 (2017).
88. Güner T, Köseoğlu D, Demir M. Multilayer design of hybrid phosphor film for application in LEDs. *Opt Mater* **60**, 422–430 (2016).
89. Lin HY, Wang SW, Lin CC et al. Effective optimization and analysis of white LED properties by using nano-honeycomb patterned phosphor film. *Opt Express* **24**, 19032–19047 (2016).
90. Lin HY, Ye ZT, Lin CC et al. Improvement of light quality by ZrO_2 film of chip on glass structure white LED. *Opt Express* **24**, A341–A352 (2016).
91. Wang WX, Yang PP, Cheng ZY et al. Patterning of red, green, and blue luminescent films based on CaWO4: Eu3+, CaWO4: Tb^{3+}, and CaWO4 phosphors via microcontact printing route. *ACS Appl Mater Interfaces* **3**, 3921–3928 (2011).
92. Chandana MR, Krushna BRR, Malleshappa J et al. Simple fabrication of novel Sm3+ doped BaGd2ZnO5 nanophosphors for flexible displays, improved data security applications, and solid-state lighting applications. *Mater Today Sustain* **22**, 100397 (2023).
93. Ru JJ, Zeng F, Zhao B et al. Development of red phosphor Li8CaLa2Ta2O13: Eu3+ for WLEDs and anti-counterfeiting applications. *ChemPhysMater* **3**, 194–203 (2024).
94. Hua Y, Kim YY, Lee SH et al. Enhanced self-host blue emission of CaSrSb2O7 materials via Bi3+ ion doping for high CRI WLEDs, security inks and flexible displays. *Mater Today Chem* **22**, 100594 (2021).
95. Hua YB, Yu JS. Dual-functional platforms toward field emission displays and novel anti-counterfeiting strategy based on rare-earth activated materials. *Ceram Int* **47**, 18003–18011 (2021).
96. Lu ZH, Luo LH, Du P et al. Ferroelectric domains and luminescent properties of Pr^{3+} -doped $Ca_2Nb_2O_7$ ceramics. *J Am Ceram Soc* **103**, 3748–3756 (2020).
97. Lu ZH, Tang J, Du P et al. Multilevel luminescence of Er^{3+}/Pr^{3+} co-doped $Ca_2Nb_2O_7$ ceramics and composite films for optical anti-counterfeiting. *Ceram Int* **47**, 8248–8255 (2021).
98. Sabri F, Allison SW, Aryal M et al. Thermal and optical characterization of up-converting thermographic phosphor polymer composite films. *MRS Adv* **3**, 3489–3494 (2018).
99. Yi SS, Jung JY. Up-conversion luminescence properties with temperature change of strontium tungstate phosphors. *RSC Adv* **12**, 24752–24759 (2022).
100. Markose KK, Anjana R, Jayaraj MK. Upconversion nanophosphors: an overview. In Jayaraj MK. *Nanostructured Metal Oxides and Devices*: *Optical and Electrical Properties* 47–102 (Springer, Singapore, 2020).
101. Sukul PP, Swart HC. Synergistic red dominancy over green upconversion studies in PbZrTiO3: Er3+/Yb3+ phosphor synthesized via two different modified technique and flexible thin-film thermometer demonstration on C1: PbZrTiO3 @PDMS substrates. *J Alloys Compd* **966**, 171656 (2023).
102. Li TS, Li X, Chi ZT et al. Stretchable phosphor/boron nitride nanosheet/polydimethylsiloxane films for thermal management and rapid monitoring. *ACS Appl Polym Mater* **4**, 1431–1439 (2022).
103. Sabri F, Lynch K, Wilson R et al. Sensing with phosphor-doped PDMS. In *IET & ISA 60th International Instrumentation Symposium 2014* 1–6 (IET, 2014); http://doi.org/10.1049/cp.2014.0539.
104. Allison SW, Sabri F, Parajuli P. Exploration of thin polymer films for phosphor thermometry. In *Proceedings of the International Instrumentation Symposium* 30–38 (2016).
105. Zhou XQ, Ning LX, Qiao JW et al. Interplay of defect levels and rare earth emission centers in multimode luminescent phosphors. *Nat Commun* **13**, 7589 (2022).
106. Sohn KS, Timilsina S, Singh SP et al. Mechanically driven luminescence in a ZnS: Cu-PDMS composite. *APL Mater* **4**, 106102 (2016).
107. Wang J, Yao KW, Cui KT et al. Contact electrification induced multicolor self-recoverable mechanoluminescent elastomer for wearable smart light-emitting devices. *Adv Opt Mater* **11**, 2203112 (2023).
108. Wu JW, Xu R, Shao MF et al. Phosphorus-based nanomaterials for biomedical applications: a review. *ACS Appl Nano Mater* **7**, 11022–11036 (2024).
109. Fang MJ, Huang SH, Li D et al. Stretchable and self-healable organometal halide perovskite nanocrystal-embedded polymer gels with enhanced luminescence stability. *Nanophotonics* **7**, 1949–1958 (2018).
110. Zhang ZY, Zong MR, Liu JR et al. Biosafety evaluation of BaSi2O2N2: Eu2+/PDMS composite elastomers. *Front Bioeng Biotechnol* **11**, 1226065 (2023).
111. Shin H, Yoon GW, Choi W et al. Miniaturized multicolor fluorescence imaging system integrated with a PDMS light-guide plate for biomedical investigation. *npj Flex Electron* **7**, 7 (2023).
112. Mollazadeh-Bajestani M, Bahmanpour A, Ghaffari M et al. Reviewing the bio-applications of SrAl2O4: Eu2+, Dy3+ phosphor. *J Biol Med* **7**, 44–52 (2023).
113. Sharma P, Bhagatji A, Tyagi S et al. Harvesting light from ZnS: Mn: Eu/PVDF mechano-luminescent composite under mechanical impact for energy conversion application. *Sens Actuators A Phys* **353**, 114197 (2023).
114. Gu Y, Lin PC, Zhang JK et al. Preparation and afterglow mechanoluminescent property of ZrO_2: Ti^{4+}/PDMS composite elastic material. *J Chin Ceram Soc* **50**, 3134 (2022).

115. Wang WX, Wang ZB, Zhang JC et al. Contact electrification induced mechanoluminescence. *Nano Energy* **94**, 106920 (2022).
116. Hua Y, Lee SH, Kim YY et al. Luminescent behavior of Eu^{2+}-doped $Ca_2YSrAlSiO$ phosphor materials for −*y*27 light-emitting diodes and security inks applications. *J Alloys Compd* **891**, 161060 (2022).
117. Hua Y, Yu JS. Recent progress in luminescent nanomaterials for next-generation displays and lighting applications. *Nanoscale* **14**, 6249–6276 (2022).
118. Kim MS, Timilsina S, Jang SM et al. A mechanoluminescent ZnS: Cu/PDMS and biocompatible piezoelectric silk fibroin/PDMS hybrid sensor for self-powered sensing and artificial intelligence control. *Adv Mater Technol* **9**, 2400255 (2024).
119. Jha P, Khare A. $SrAl_2O_4$: Eu, Dy mechanoluminescent flexible film for impact sensors. *J Alloys Compd* **847**, 156428 (2020).
120. Kong K, Dyer K, Weaver PM et al. Experimental characterisation and micromechanical models for luminescent phosphors incorporated with nonwoven veil-polymer composites. *Compos B: Eng* **202**, 108444 (2020).
121. Wang HJ, Chen XM, Tian Z et al. Efficient color manipulation of zinc sulfide-based mechanoluminescent elastomers for visualized sensing and anti-counterfeiting. *J Lumin* **228**, 117590 (2020).
122. Krishnan S, Katsube N, Sundaresan V. Finite strain elasticity based cohesive zone model for mechanoluminescent composite interface: I. Stiffness of the undamaged interface. *Smart Mater Struct* **30**, 015016 (2020).
123. Cheng Q, Wang Y, Su L et al. Wide-spectrum manipulation of triboelectrification-induced electroluminescence by long afterglow phosphors in elastomeric zinc sulfide composites. *J Mater Chem C* **7**, 4567–4572 (2019).
124. Krishnan S, Vijayaraghavan P, Sundaresan V. Characterization of mechanoluminescent composites and their applications for SHM of polymer composites. In *ASME 2015 Conference on Smart Materials*, *Adaptive Structures and Intelligent Systems* (ASME, 2015); https://doi.org/10.1115/SMASIS2015-9078.
125. Chen L, Wong MC, Bai GX et al. White and green light emissions of flexible polymer composites under electric field and multiple strains. *Nano Energy* **14**, 372–381 (2015).
126. Hao SN, Oi YH, Zhang ZP. Settlement behavior and mechanism of *Navicula* sp. on WLAP/PDMS composite coating under simulative diurnal alternation, constant light and dark conditions. *Surf Interfaces* **42**, 103527 (2023).
127. Xia WX, Cheng H, Mao QN et al. Improving the luminescence performance of far-red-emitting Sr2ScSbO6: Mn4+ phosphor with charge compensation and its application in plant growth LEDs. *Ceram Int* **49**, 13708–13716 (2023).
128. Kang ZY, Wang SC, Seto T et al. A highly efficient Eu^{2+} excited phosphor with luminescence tunable in visible range and its applications for plant growth. *Adv Opt Mater* **9**, 2101173 (2021).
129. Yang CX, Liu W, You Q et al. Recent advances in light-conversion phosphors for plant growth and strategies for the modulation of photoluminescence properties. *Nanomaterials* **13**, 1715 (2023).
130. Wen L, Liu NS, Wang SL et al. Enhancing light emission in flexible ac electroluminescent devices by tetrapod-like zinc oxide whiskers. *Opt Express* **24**, 23419–23428 (2016).
131. Kim T, Kim HS. Color change in mixed zinc sulfide composite displays due to a biased AC electric field. *New Phys Sae Mulli* **73**, 658–663 (2023).
132. Vitasek J, Jargus J, Hejduk S et al. Phosphor decay measurement and its influence on communication properties. In *2017 19th International Conference on Transparent Optical Networks* (*ICTON*) 1–4 (IEEE, 2017); http://doi.org/10.1109/ICTON.2017.8024951.
133. Saah FK, Gbawoquiya FL, Chaudhary R et al. Green synthesis of carbon quantum dots for detecting heavy metal ionsin environmental samples. *High Technol Lett* **29**, 174–205 (2023).
134. YUE Y,GUO L C,LIU H Z,et al. Multimode X-ray Detection of Double Perovskite Ba_2LuNbO_6：Tb^{3+}Scintillators. *Chinese Journal of Luminescence* **44**, 1597–1605 (2023).
135. Xie LY, Kang J, Han MX et al. pH sensor based on PDMS fiber doped by NaBaScSi2O7: Eu^{2+}. In *2023 21st International Conference on Optical Communications and Networks (ICOCN)* 1–3 (IEEE, 2023); http://doi.org/10.1109/ICOCN59242.2023.10236433.
136. Kałużna-Czaplińska J, Gątarek P, Chirumbolo S et al. How important is tryptophan in human health?. *Crit Rev Food Sci Nutr* **59**, 72–88 (2019).
137. Carrillo-Betancourt RA, Hernández-Cordero J. Polymer coatings with rare-earth activated phosphors for optical fiber fluorosensors. *Proc SPIE* **12202**, 122020B (2022).
138. Wang ZJ, Liu JQ, Feng YP et al. Hydrothermal synthesis of hexagonal-like YvO_4: Eu^{3+} microcrystals and their fluorescence properties. *J Alloys Compd* **580**, 500–504 (2013).
139. Wang F, Chen LF, Zhu JM et al. A phosphorescence quenching-based intelligent dissolved oxygen sensor on an optofluidic platform. *Micromachines (Basel)* **12**, 281 (2021).
140. Gouin S, Gouterman M. Ideality of pressure-sensitive paint. II. Effect of annealing on the temperature dependence of the luminescence. *J Appl Polym Sci* **77**, 2805–2814 (2000).
141. Xiong G, Zhang ZP, Zhang C et al. SLAP@g-C_3N_4 fluorescent photocatalytic composite powders enhance the anti-bacteria adhesion performance and mechanism of polydimethylsiloxane coatings. *Nanomaterials* **12**, 3005 (2022).
142. Hao SN, Qi YH, Zhang ZP. Influence of light conditions on the antibacterial performance and mechanism of waterborne fluorescent coatings based on waterproof long afterglow phosphors/PDMS composites. *Polymers* **15**, 3873 (2023).
143. Xiong G, Zhang ZP, Qi YH. Effect of the properties of long afterglow phosphors on the antifouling performance of silicone fouling-release coating. *Prog Org Coat* **170**, 106965 (2022).
144. Jin HC, Bing W, Jin E et al. Bioinspired PDMS–phosphor–silicone rubber sandwich-structure coatings for combating biofouling. *Adv Mater Interfaces* **7**, 1901577 (2020).
145. Yang LN, Liu B, Wang YH et al. Novel double light-color (blue and red) phosphor Sr9Ca(Li, Na, K)(PO4)7: Eu2+ excited by NUV light for outdoor plant cultivation. *Adv Mater Technol* **9**, 2301751 (2024).
146. Jia MY, Kim TJ, Yang Y et al. Automated multi-parameter high-dose-rate brachytherapy quality assurance via radioluminescence imaging. *Phys Med Biol* **65**, 225005 (2020).
147. Ibru T, Mohan K, Antoniou A. Physical properties of elastomer composites with scintillating additives. *Sens Actuators A Phys* **280**, 383–389 (2018).
148. Allison SW, Baker ES, Lynch KJ et al. In vivo x-ray imaging of phosphor-doped PDMS and phosphor-doped aerogel biomate-

rials. *Int J Polym Mater Polym Biomater* **64**, 823–830 (2015).

149. Wen Q, Yang JL, Li SR et al. Micropatterning of lanthanide complex species onto self-cracking flexible transparent films and their photophysical properties. *Mater Res Bull* **88**, 98–104 (2017).
150. Wi JH, Jung JY, Park SG. Synthesis of rare-earth-doped strontium tungstate phosphor at room temperature and applied flexible composite. *Materials* **15**, 8922 (2022).
151. Yi SS, Jung JY. Barium molybdate white emitting phosphor synthesized at room temperature by co-precipitation. *RSC Adv* **12**, 21827–21835 (2022).
152. Murai S, Inoue Y, Tanaka K. Fabrication of flexible sticker of Si metasurfaces by a transfer process. *J Jpn Soc Powder Powder Metall* **69**, 87–90 (2022).
153. Zheng JH, Mehrvarz H, Liao C et al. Large-area 23%-efficient monolithic perovskite/homojunction-silicon tandem solar cell with enhanced UV stability using down-shifting material. *ACS Energy Lett* **4**, 2623–2631 (2019).
154. Qu BY, Jiao YC, He SW et al. Improved performance of a-Si: H solar cell by using up-conversion phosphors. *J Alloys Compd* **658**, 848–853 (2016).
155. Li JX, Zuo C, Chen J M et al. Effect of phosphor carriers on fluorescence of ruthenium phenanthroline and performance of oxygen-sensitive fluorescent membranes. *Imaging Sci Photochem* **33**, 211–217 (2015).
156. Leal-Junior A, Avellar L, Biazi V et al. Multifunctional flexible optical waveguide sensor: on the bioinspiration for ultrasensitive sensors development. *Opto-Electron Adv* **5**, 210098 (2022).
157. Zhang L, Pan J, Zhang Z et al. Ultrasensitive skin-like wearable optical sensors based on glass micro/nanofibers. *Opto-Electron Adv* **3**, 190022 (2020).

Acknowledgements

The research was co-funded by the financial support of the European Union under the REFRESH – Research Excellence For REgion Sustainability and High-tech Industries project number CZ.10.03.01/00/22003/0000048 via the Operational Programme Just Transition. This work was also supported by the Ministry of Education, Youth, and Sports of the Czech Republic conducted by the VSB-Technical University of Ostrava, under grant no. SP2024/081. This work was developed within the scope of the projects CICECO (LA/P/0006/2020, UIDB/50011/2020 & UIDP/50011/2020) and DigiAqua (PTDC/EEI-EEE/0415/2021), financed by national funds through the (Portuguese Science and Technology Foundation/MCTES (FCT I.P.)).

Competing interests

The authors declare no competing financial interests.

Scan for Article PDF